

**A Software Platform For The Simulation Of Light Propagation In
Photonic Crystal Structures With Defects**

Santiago Echeverri Chacón

sechev14@eafit.edu.co

Advisor: Nicolás Guarín Zapata

nicoguarin@gmail.com

Departamento de Ciencias Básicas

Escuela de Ciencias y Humanidades

Universidad EAFIT

Medellín Colombia

May 2013

**A Software Platform For The Simulation Of Light Propagation In
Photonic Crystal Structures With Defects**

Santiago Echeverri Chacón
sechev14@eafit.edu.co

Advisor: Nicolás Guarín Zapata
nicoguarin@gmail.com

Thesis document presented as a partial prerequisite for the title of
Bachelor in Engineering Physics

Departamento de Ciencias Básicas
Escuela de Ciencias y Humanidades
Universidad EAFIT
Medellín Colombia
May 2013

Contents

| | | |
|----------|--|-----------|
| 1 | Introduction | 5 |
| 2 | Problem | 7 |
| 2.1 | Problem statement | 7 |
| 2.2 | Objectives | 7 |
| 2.2.1 | General objectives | 7 |
| 2.3 | Justification | 8 |
| 3 | Electromagnetic waves in periodic media | 11 |
| 3.1 | Maxwell equations | 11 |
| 3.2 | Wave equation for electric fields | 13 |
| 3.3 | Time harmonic fields, reciprocal space and Fourier transform | 14 |
| 3.4 | Electromagnetism as an eigenvalue problem | 15 |
| 3.4.1 | Hermiticity | 16 |
| 3.4.2 | Symmetry groups | 17 |
| 3.4.3 | Conservation of energy for waves in source less media | 19 |
| 3.4.4 | Energy functional of electromagnetic waves | 19 |
| 4 | Finite element method | 21 |
| 4.1 | Weak formulation of the problem | 22 |
| 4.2 | Boundary conditions | 23 |

| | | |
|----------|---|-----------|
| 4.3 | Abstract form of the equation | 24 |
| 4.4 | Base functions and discretization | 24 |
| 4.5 | Vectorial vs scalar formulation | 30 |
| 4.6 | Edge elements vs Node Elements | 30 |
| 4.7 | Second order elements, shape functions. | 30 |
| 4.8 | Numerical integration and Gauss quadrature | 30 |
| 4.9 | Mass matrices | 30 |
| 4.10 | Explicit formulation | 30 |
| 5 | Implementation | 33 |
| 5.1 | Object Oriented Paradigm | 33 |
| 5.2 | Classes, Diagrams and flow charts of PeYeQM | 33 |
| 6 | Results | 35 |
| 6.1 | Electrostatic benchmark tests | 35 |
| 6.1.1 | Electric field due to charged elements | 35 |
| 6.2 | Harmonic benchmark tests | 41 |
| 6.2.1 | Eigenvalues and modes in waveguides | 41 |
| 6.2.2 | Bloch periodic lattices and dispersion curves | 46 |
| 7 | Conclusions and future work | 51 |
| 7.1 | Conclusions | 51 |
| 7.2 | Future work | 52 |

Chapter 1

Introduction

^{c1} Preface:

Definition of the problem will be treated in chapter 2, followed by a brief state of the art recollection where some background in the topics of photonic crystals and computational methods for physics will be mentioned. Then, fundamental concepts behind light propagation in periodic materials (chapter 3) and the model used for the finite element procedure used are presented.

^{c1} NGZ: La introducción es lo que motiva al lector a leer el documento. Debe responder las preguntas: Por qué es relevante esto?, Por qué es relevante que yo (como ingeniero físico) lo haya abordado?, Qué componentes de ingeniería y de física se han tocado en el trabajo?

Chapter 2

Problem

2.1 Problem statement

This project aims to develop a simulation software package that permits analysis of electromagnetic (EM) wave propagation, in the context of Photonic Crystal (PC) defects modelling and design.

2.2 Objectives

2.2.1 General objectives

- Build a software platform capable of simulating electromagnetic field propagation in perfect PC and also in PC with defects such as cavities and inclusions.
- The platform architecture must be structured in a way that facilitates future upgrading, possible optimization schemes, and integration with other kinds of simulations like confinement of electrons in potential wells and crystals.

Specific objectives

1. Apprehend the theory behind EM fields and its applications in photonics. Particularly:
 - (a) general overview of computational methods in electromagnetism and deeper understanding of methods that fit the problem statement.
 - (b) Photonic crystals and the mathematical tools for modeling periodicity, as well as
 - (c) technological applications of defects in photonic crystals and common case studies.

2. Define a set of implementation requirements and constraints, in terms of the numerical method, and expected functionality.
3. Implement algorithms to solve problems that relate to technological applications studied in the appropriation stage.
 - (a) Solve simple scalar-static 2D problems
 - (b) Implement vector field solver for stationary non periodic conditions (this may qualify as spectral solution or not)
 - (c) Vector field solutions for time dependent problems
 - (d) Introduce periodic conditions
4. Document and share the results of the simulations making an analysis of the relevance and feasibility of the platform.

2.3 Justification

Most of the artificial environment we as a society have built to live in, is in one way or another a consequence of our ability to understand and transform materials present in nature. This understanding is so important that human history studies have come to address cultural stages of our evolution from: the Stone Age through Bronze Age, as the materials we used to overcome survival challenges [13]. Even in recent years, extraordinary changes in the way we evolve as a species can be attributed to achievements only possible by improvements on our understanding of material properties. Take for example the paradigm change caused by the discovery of electronic properties of materials such as semiconductors [18]. And the ever growing stream of technological applications derived from it.

The next frontier in the context of material science, relies in a level of understanding that allows us to not only use and transform materials, but to design them. This is the field of metamaterials, a field in which by means of manipulating the microscopical structure and geometry of a crystal-like solid, we can obtain macroscopic properties that are otherwise impossible to find in nature [7, 3]. One of the sub domains of the metamaterials frontier is that of media capable of molding and manipulating electromagnetic waves. The ability to harness light has the prospect to support a new technological revolution of a scale similar to that of transistor revolution [13]. Advances in engineered optical materials will benefit the development of areas such as high speed computing, spectroscopy, laser engineering, biomedicine and quantum computing [18]. This project concerns about one candidate of optical metamaterial set known as photonic crystals, and particularly, the light guiding properties that arise when taking advantage of lattice cavities. Photonic crystals are:

“Artificially created periodic low-loss dielectric medium in which electromagnetic waves of certain frequencies cannot propagate [8]”.

2.3. JUSTIFICATION

9

Light in that certain frequency gap is virtually stopped because of periodicity of dielectric dispersers and the destructive interference that arises from it. This property is used in technical application for many forms of technological developments. For example Kärtner's et al. developed high resolution PC based Analogic-Digital (AD) conversion circuits [14] that are showing all-optical circuits which outperform electronic based components. Telecommunications also benefit from technologies such as ultra low loss photonic crystal fibers [2]. As well as low cost, and high definition spectroscopy technologies that take advantage of spectral selectivity in PCs; Pervez [20] has used a phenomenon called outcoupling to fabricate cheap PC based spectrometers. On the other hand, a lot of effort has been made to exploit the light confinement properties of PCs to make micro laser cavities and even single-photon sources. Theoretical background and numerical studies on spontaneous emission using microcavities in PCs has been undertaken by many researchers including works from Yablonovich and Vileneuve [33, 32, 30]. Experimental measures of ultrafast nanocavity lasers was performed by Hatice [1] in 2006, and Moore [17] in 2008. Even state of the art quantum computing experiments are being possible by using PC based waveguides and cavities as shown by Wolters in [31].

The nature of most PC application problems, is of such complexity that very often numerical tools are the only way of modeling new designs and performance. Figure 2.1 shows some of the fields that benefit from electromagnetic numerical simulations as stated by Jin [12]. Computational methods such as: Plane Wave Expansion (PWE) [27, 15], Finite Difference Time Domain (FDTD) [2, 19], Method of Moments (MoM) or Boundary Element Method (BEM) and Finite Element Methods (FEM)[25, 16], have had their share in the modeling of electromagnetic fields under many different scenarios. Every one of them having their own strengths and weaknesses in terms of: ease of implementation, precision, and computational resources.

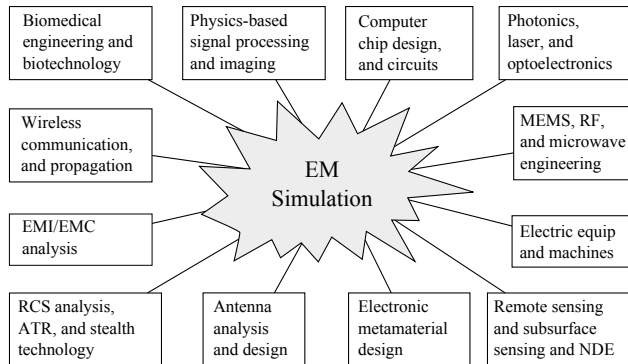


Figure 2.1: Maxwell equations by the hand of numerical methods have the power to impact many scientific and technological areas. Taken from Jin et al [12]

In the context of Universidad EAFIT, and specifically of Engineering Physics, we see a growing research background in computational physics that goes from modeling seismic waves [10], and resonant modes in musical instruments [24]; passing through quantum mechanics like relativistic phenomena in graphene [29], and quantum potential wells and crystals [6]; to finally address

a computational module for digital holography and speckle [26], and research on Plane Wave Methods for calculation of bandgap structures in photonic crystals [15]. It can be stated that this trend in numerical methods applied to crystal-like materials has been embraced and supported by the Computational and Theoretical Physics Research Initiative of engineering physics students (SFTyC). This work expands and continues the initiative towards strengthening undergraduate research and software development abilities.

Chapter 3

Electromagnetic waves in periodic media

c1

3.1 Maxwell equations

Give an introduction to Maxwell equations in both their Integral and Differential forms.

$$\oint_C \mathbf{E} \cdot d\mathbf{l} = -\frac{d}{dt} \int_S \mathbf{B} \cdot d\mathbf{S} \quad (\text{Faraday}) \quad (3.1)$$

$$\oint_C \mathbf{H} \cdot d\mathbf{l} = \frac{d}{dt} \int_S \mathbf{D} \cdot d\mathbf{S} + \int_S \mathbf{J} \cdot d\mathbf{S} \quad (\text{Ampere-Maxwell}) \quad (3.2)$$

$$\int_S \mathbf{D} \cdot d\mathbf{S} = \int_V \rho dV \quad (\text{Gauss}) \quad (3.3)$$

$$\int_S \mathbf{B} \cdot d\mathbf{S} = 0 \quad (\text{Gauss for magnetism}), \quad (3.4)$$

^{c1} NGZ: Falta una intro a este capitulo: Que se describe en este capitulo?

In differential form we have

$$\nabla \times \mathbf{E} = -\frac{\partial \mathbf{B}}{\partial t} \quad (\text{Faraday}) \quad (3.5)$$

$$\nabla \times \mathbf{H} = \frac{\partial \mathbf{D}}{\partial t} + \mathbf{J} \quad (\text{Ampere-Maxwell}) \quad (3.6)$$

$$\nabla \cdot \mathbf{D} = \rho \quad (\text{Gauss}) \quad (3.7)$$

$$\nabla \cdot \mathbf{B} = 0 \quad (\text{Gauss for magnetism}) \quad (3.8)$$

$$\nabla \cdot \mathbf{J} = -\frac{\partial \rho}{\partial t} \quad (\text{Continuity}), \quad (3.9)$$

Describe the current Continuity Equation

$$\int_S \mathbf{J} \cdot d\mathbf{S} = -\frac{d}{dt} \int_V \rho dV. \quad (3.10)$$

from (3.5) to (3.9) we can get just 3 independent set of vectorial equations. Define the meaning of each variable in that expression and continue with the definition of constitutive relations (Electric polarization and Magnetization):

In both set of equation we have

- \mathbf{E} : Electric field intensity (volts/meter),
- \mathbf{D} : Electric flux density (coulombs/meter²),
- \mathbf{H} : Magnetic field intensity (amperes/meter),
- \mathbf{B} : Magnetic flux density (webers/meter),
- \mathbf{J} : Electric current density (amperes/meter²),
- ρ : Electric charge density (coulombs/meter³).

$$\mathbf{D} = \epsilon_0 \cdot \mathbf{E} + \mathbf{P} \quad (3.11)$$

$$\mathbf{B} = \mu_0 \cdot \mathbf{H} + \mathbf{M}, \quad (3.12)$$

\mathbf{P} is the polarization vector that tell us information about the response of the material to the external field due to orientation of the molecules inside of it, and \mathbf{M} is the magnetization vector that is the analogous of the polarization for the magnetic case. If the fields are small enough the behavior of the material is linear and we can express the polarization and magnetization vectors as linear functions of \mathbf{E} and \mathbf{H}

$$\mathbf{D} = \bar{\epsilon} \cdot \mathbf{E} \quad (3.13)$$

$$\mathbf{B} = \bar{\mu} \cdot \mathbf{H}, \quad (3.14)$$

where the double bar refers to a second order tensor, \cdot is a tensor-vector product.

This may be a good place to talk about classification of media and or boundary conditions, Jian-mings book: Theory and computation of electromagnetic fields might be a good source for that.

3.2 Wave equation for electric fields

If we take the curl to (3.5), we get

$$\nabla \times \nabla \times \mathbf{E} = -\frac{\partial}{\partial t} \nabla \times \mathbf{B} = -\frac{\partial}{\partial t} \nabla \times (\bar{\mu} \cdot \mathbf{H}) ,$$

assuming a (piecewise) homogeneous material

$$\begin{aligned} \nabla \times \nabla \times \mathbf{E} &= -\frac{\partial}{\partial t} \nabla \times \mathbf{B} = \frac{\partial}{\partial t} (\bar{\mu} \cdot \nabla \times \mathbf{H}) \\ &= -\frac{\partial}{\partial t} \left(\bar{\mu} \cdot \left[\frac{\partial \mathbf{D}}{\partial t} + \mathbf{J} \right] \right) , \end{aligned}$$

if the polarization and magnetization do not vary with time –there is not hysteresis–

$$\begin{aligned} \nabla \times \nabla \times \mathbf{E} &= -\bar{\mu} \cdot \left[\frac{\partial^2 \mathbf{D}}{\partial t^2} + \frac{\partial \mathbf{J}}{\partial t} \right] \\ \nabla \times \nabla \times \mathbf{E} &= -\bar{\mu} \cdot \left[\bar{\epsilon} \cdot \frac{\partial^2 \mathbf{E}}{\partial t^2} + \frac{\partial \mathbf{J}}{\partial t} \right] . \end{aligned} \quad (3.15)$$

Similarly, we take the curl to (3.6), and under the same assumptions, we get

$$\begin{aligned} \nabla \times \nabla \times \mathbf{H} &= \frac{\partial \nabla \times \mathbf{D}}{\partial t} + \nabla \times \mathbf{J} \\ &= \frac{\partial \nabla \times (\bar{\epsilon} \cdot \mathbf{E})}{\partial t} + \nabla \times \mathbf{J} \\ &= \frac{\partial \bar{\epsilon} \cdot \nabla \times \mathbf{E}}{\partial t} + \nabla \times \mathbf{J} \\ &= \frac{\partial \bar{\epsilon} \cdot (-\frac{\partial \mathbf{B}}{\partial t})}{\partial t} + \nabla \times \mathbf{J} , \end{aligned}$$

finally

$$\begin{aligned} \nabla \times \nabla \times \mathbf{H} &= -\bar{\epsilon} \cdot \frac{\partial^2 \mathbf{B}}{\partial t^2} + \nabla \times \mathbf{J} \\ \nabla \times \nabla \times \mathbf{H} &= -\bar{\epsilon} \cdot \bar{\mu} \cdot \frac{\partial^2 \mathbf{H}}{\partial t^2} + \nabla \times \mathbf{J} . \end{aligned} \quad (3.16)$$

If we apply the vector identity $\nabla \times \nabla \times \mathbf{A} = \nabla(\nabla \cdot \mathbf{A}) - \nabla^2 \mathbf{A}$, and assume that we do not have electrical charges^{c0} we can rewrite (3.15) and (3.16) as

$$\nabla^2 \mathbf{E} = \bar{\mu} \cdot \bar{\epsilon} \cdot \frac{\partial^2 \mathbf{E}}{\partial t^2} - \bar{\mu} \cdot \frac{\partial \mathbf{J}}{\partial t} \quad (3.17)$$

$$\nabla^2 \mathbf{H} = \bar{\epsilon} \cdot \bar{\mu} \cdot \frac{\partial^2 \mathbf{H}}{\partial t^2} - \nabla \times \mathbf{J} \quad (3.18)$$

If we neglect the terms $\frac{\partial \mathbf{J}}{\partial t}$ and $\nabla \times \mathbf{J}$ –the source terms in the equations– and assume isotropy –assuming isotropy the material tensors could be represented as simple scalars– we get the well known expressions

$$\left(\nabla^2 - \mu \epsilon \frac{\partial^2}{\partial t^2} \right) \mathbf{E} = \mathbf{0} \quad (3.19)$$

$$\left(\nabla^2 - \mu \epsilon \frac{\partial^2}{\partial t^2} \right) \mathbf{H} = \mathbf{0} , \quad (3.20)$$

that are vectorial wave equations with phase speed $c = \sqrt{\epsilon \mu}$.

This form of (3.15) is relevant for us because the program is currently based on this approximation. This particular topic will be treated furthermore in the implementation section ??.

3.3 Time harmonic fields, reciprocal space and Fourier transform

Linearity of Maxwell equations, and a restriction to time harmonic variations permits the separation of time and spatial dependencies in the form:

$$\mathbf{E}(\mathbf{r}, t) = \mathbf{E}(\mathbf{r}) e^{-i\omega t}$$

This is known as a phasorial notation, and from here on, when dealing with time harmonic fields we will be interested only on the unknown phasor function $\mathbf{E}(\mathbf{r})$ which will represent the field distribution at a fixed time.

Considering a single harmonic wave propagating with angular frequency ω we get:

$$\nabla \times \nabla \times \mathbf{E} = -\omega^2 \bar{\mu} \cdot \bar{\epsilon} \cdot \mathbf{E} - i\omega \bar{\mu} \cdot \mathbf{J} \quad (3.21)$$

$$\nabla \times \nabla \times \mathbf{H} = -\omega^2 \bar{\epsilon} \cdot \bar{\mu} \cdot \mathbf{H} + \nabla \times \mathbf{J} , \quad (3.22)$$

^{c0}This identity always hold for the magnetic field since it is divergence free. WHAT ABOUT THE ELECTRICAL CASE?? Maybe this is why Joannopolous treats the problem for the magnetic field case instead of the electric one
^{c1}

that are the expressions for the frequency domain.

$$\bar{\mu} = \mu_0 \bar{\mu}_r \quad (3.23)$$

$$\bar{\epsilon} = \epsilon_0 \bar{\epsilon}_r \quad (3.24)$$

$$\mu_0 = \sqrt{\mu_0 \epsilon_0} \sqrt{\frac{\mu_0}{\epsilon_0}} \quad (3.25)$$

$$k_0 = \omega \sqrt{\mu_0 \epsilon_0} \quad (3.26)$$

$$Z_0 = \sqrt{\frac{\mu_0}{\epsilon_0}} \quad (3.27)$$

$$c = \frac{1}{\sqrt{\mu_0 \epsilon_0}} \quad (3.28)$$

where $\bar{\mu}_r, \bar{\epsilon}_r$ are the relative permeability and permittivity, respectively, k_0 , Z_0 , and c are the free space wave number intrinsic impedance, and speed of light in free space. Using this:

$$\bar{\mu}_r^{-1} \nabla \times \nabla \times \mathbf{E} = -\omega^2 \mu_0 \epsilon_0 \bar{\epsilon}_r \cdot \mathbf{E} - i\omega \mu_0 \mathbf{J} \quad (3.29)$$

$$\bar{\mu}_r^{-1} \nabla \times \nabla \times \mathbf{E} = k_0^2 \bar{\epsilon}_r \cdot \mathbf{E} - ik_0 Z_0 \mathbf{J} \quad (3.30)$$

3.4 Electromagnetism as an eigenvalue problem

The current section treats the harmonic wave equation in a formalism similar to that of quantum mechanics. It might be seen as a summarized version of the treatment of Joannopoulos [13], and Johnson.^{c1}

Going back to equation 3.30, and assuming no sinks or sources ($\mathbf{J} = 0$), we can see that the form of the equation is one of a eigenvalue problem. Where a series of operations on a function \mathbf{E} (eigenfunction or eigenvector) gives us the same function multiplied by a constant scalar (eigenvalue). In this case we will label the operator acting on \mathbf{E} as $\hat{\Theta}$ in order to make the equation look like a simpler-looking eigenvalue problem:

$$\hat{\Theta} \mathbf{E} = \left(\frac{\omega}{c} \right)^2 \mathbf{E} \quad (3.31)$$

Where:

$$\hat{\Theta} \mathbf{E} \triangleq \bar{\mu}_r^{-1} \nabla \times \nabla \times \mathbf{E} \quad (3.32)$$

^{c1} NGZ: Entre este párrafo y el siguiente hace falta una mejor conexión.

Here the eigenvectors or phasors \mathbf{E} represent spatial patterns of the harmonic modes, and eigenvalues $(\frac{\omega}{c})^2$ give information about the frequency ω (and thus wave number k_0) of such modes.

3.4.1 Hermiticity

As in Quantum Mechanics with the Hamiltonian, some key properties of the eigenfunctions that satisfy equation 3.31 are ^{c0}:

- Have real eigenvalues,
- are orthogonal,
- can be obtained by a variational principle
- and can be catalogued by symmetry properties .

All of these properties rely on the fact that the linear operator is from a kind known as **Hermitian operator**.

To understand why $\hat{\Theta}$ is Hermitian we need first to understand the inner product of two wavefunctions $\mathbf{F}(\mathbf{r})$ and $\mathbf{G}(\mathbf{r})$:

$$(\mathbf{F}(\mathbf{r}), \mathbf{G}(\mathbf{r})) \triangleq \int \mathbf{F}^*(\mathbf{r}) \cdot \mathbf{G}(\mathbf{r}) \quad (3.33)$$

where $*$ denotes complex conjugation. From definition 3.33 we can see that: $(\mathbf{F}, \mathbf{G}) = (\mathbf{G}, \mathbf{F})^*$ for and \mathbf{F} and \mathbf{G} . Also, (\mathbf{F}, \mathbf{F}) is always real and non-negative, and (\mathbf{F}, \mathbf{F}) is known as the L^2 norm of \mathbf{F} . A normalized wavefunction is one where $(\mathbf{F}, \mathbf{F}) = 1$.

Having defined an inner product for two wavefunctions, we say that any operator $\hat{\Theta}$ is **Hermitian** if $(\mathbf{F}, \hat{\Theta}\mathbf{G}) = (\hat{\Theta}\mathbf{F}, \mathbf{G})$ for any fields \mathbf{F} and \mathbf{G} .

Now using this we can check that the operator in equation 3.30 is Hermitian and derive nice properties around that conclusion:

^{c0}This proposition holds if we are not considering lossy materials, where the properties are treated as complex valued tensor and then the matrix is no longer Hermitian.

$$\begin{aligned}
(\mathbf{F}, \hat{\Theta} \mathbf{G}) &= \int \mathbf{F}^* \cdot \frac{1}{\bar{\mu}_r} \nabla \times \nabla \times \mathbf{G} \\
&= \int (\nabla \times \mathbf{F})^* \cdot \frac{1}{\bar{\mu}_r} (\nabla \times \mathbf{G}) + \int \nabla \cdot \left(\mathbf{F} \times \frac{1}{\bar{\mu}_r} \nabla \times \mathbf{G} \right) \\
&= \int \left[\nabla \times \left(\frac{1}{\bar{\mu}_r} \nabla \times \mathbf{F} \right) \right]^* \cdot \mathbf{G} + \int \nabla \cdot \left(\nabla \times \mathbf{F} \times \frac{1}{\bar{\mu}_r} \nabla \times \mathbf{G} \right) + \int \nabla \cdot \left(\mathbf{F} \times \frac{1}{\bar{\mu}_r} \nabla \times \mathbf{G} \right) \\
&= \int \left[\nabla \times \left(\frac{1}{\bar{\mu}_r} \nabla \times \mathbf{F} \right) \right]^* \cdot \mathbf{G} \\
&= (\hat{\Theta} \mathbf{F}, \mathbf{G})
\end{aligned}$$

Here the vector cross product identity^{c0} is used twice and surface terms that derive from using the Divergence Theorem are neglected.

The importance of knowing that the operator in the left side of 3.30 is hermitian resides in the fact that Hermitian operators have real numbers as eigenvalues. This can be seen by taking the inner product $(\mathbf{E}, \hat{\Theta} \mathbf{E})$ and observing that operation of $\hat{\Theta}$ on one of its eigenvectors \mathbf{E} produces the same eigenvector multiplied by the eigenvalue as shown in 3.31. Then:

$$(\mathbf{E}, \hat{\Theta} \mathbf{E}) = \left(\frac{\omega}{c} \right)^2 (\mathbf{E}, \mathbf{E})$$

Given that (\mathbf{E}, \mathbf{E}) is real, as we mentioned before, when taking the complex conjugate of that product we have:

$$(\mathbf{E}, \hat{\Theta} \mathbf{E})^* = \left(\frac{\omega^2}{c^2} \right)^* (\mathbf{E}, \mathbf{E})$$

and being Hermitian:

$$\begin{aligned}
(\mathbf{E}, \hat{\Theta} \mathbf{E})^* &= (\mathbf{E}, \hat{\Theta} \mathbf{E})^* \\
\left(\frac{\omega^2}{c^2} \right)^* (\mathbf{E}, \mathbf{E}) &= \left(\frac{\omega^2}{c^2} \right) (\mathbf{E}, \mathbf{E})
\end{aligned}$$

Speed of light c is real, so $\omega^2 = (\omega^2)^*$ must be real.

3.4.2 Symmetry groups

As in Quantum Mechanics and any other eigen-problems, we must introduce the concept of orthogonality in order to understand other operations. We say that two wavevectors are **orthogonal** if $(\mathbf{E}, \mathbf{E}) = 0$, and this happens whenever they have different frequencies. This can be seen as a product of Hermiticity of operator $\hat{\Theta}$ by the following operation on two different modes \mathbf{E}_1 and

^{c0} $\nabla \cdot (\mathbf{A} \times \mathbf{B}) = \mathbf{B} \cdot (\nabla \times \mathbf{A}) - \mathbf{A} \cdot (\nabla \times \mathbf{B})$ With $\mathbf{A} = \mathbf{F}$ and $\mathbf{B} = \nabla \times \mathbf{G}$, first and then $\mathbf{A} = \nabla \times \mathbf{F}$ and $\mathbf{B} = \mathbf{G}$

\mathbf{E}_1 :

$$\begin{aligned} c^2 (\mathbf{E}_2, \hat{\Theta} \mathbf{E}_1) &= c^2 (\hat{\Theta} \mathbf{E}_2, \mathbf{E}_1) \\ \omega_1^2 (\mathbf{E}_2, \mathbf{E}_1) &= \omega_2^2 (\mathbf{E}_2, \mathbf{E}_1) \\ (\omega_1^2 - \omega_2^2) (\mathbf{E}_2, \mathbf{E}_1) &= 0 \end{aligned}$$

From this one can see that if two eigenfunctions have different frequencies ($\omega_1^2 - \omega_2^2 \neq 0$) then $(\mathbf{E}, \mathbf{E}) = 0$ must be true and they are orthogonal. Now, if $(\omega_1^2 - \omega_2^2) = 0$ then \mathbf{E}_1 and \mathbf{E}_2 are not necessarily orthogonal, and the value is known as a **degenerate** frequency because there is more than one state or wavefunction with eigenvalue $\left(\frac{\omega^2}{c^2}\right)$. In this section we will see that degeneracy is related with symmetries of the domain, and that will be useful for the solution of periodic problems.

Symmetry operations are operations that do not transform the wavefunction of a mode. Symmetries of a problem are such that if a symmetry operation is applied to the wavefunction, it remains the same but multiplied by a scalar. This is called being invariant under the operation. So rotation, inversion, and reflections, are common symmetry operations that can be applied to systems that are symmetric under rotation, inversion and reflection, respectively. Probably the most immediate symmetry operation one can think of is the identity operation: $\hat{E}\mathbf{E}(\mathbf{r}) = \mathbf{E}(\mathbf{r})$, that transform a system into itself.

Another interesting operation is that of Inversion (\hat{O}_I), which takes a function $\mathbf{E}(\mathbf{r})$ and inverts its argument: $\hat{O}_I \mathbf{E}(\mathbf{r}) = \mathbf{E}(-\mathbf{r})$. If $\mathbf{E}(-\mathbf{r}) = \mathbf{E}(\mathbf{r})$ we say that the mode is invariant under inversion, or invertible. Finally, the translation operator is one where the argument gets shifted in space by a given displacement \mathbf{d} : $\hat{T}_d \mathbf{E}(\mathbf{r}) = \mathbf{E}(\mathbf{r} - \mathbf{d})$. One function that is invariant over translation operations is a plane wave like e^{ikz} , because operation of \hat{T} over the planewave gives the same wavefunction by a scalar $e^{-ik\mathbf{d}}$:

$$\hat{T} e^{ikz} = e^{ik(z-\mathbf{d})} = e^{-ik\mathbf{d}} e^{ikz}$$

We can see here that this is an eigenvalue problem with eigenfunctions of the form e^{ikz} and complex eigenvalues $e^{-ik\mathbf{d}}$. Now, operators can act on other operators, and they can also be invariant under symmetry operations. If we have an operator $\hat{\Theta}$ whose intrinsic medium properties are characterized by $\bar{\epsilon}$ and $\bar{\mu}$, and those properties are homogeneous in space, we will be acting on a system with translational symmetry. That is, the operator is the same at different points in space. So, if we have a wave function $\mathbf{E}(\mathbf{r})$ displace it with \hat{T}_d , then act on it with $\hat{\Theta}$ and displace it back with an inverted translation operator \hat{T}_d^{-1} we will get the same result as if only $\hat{\Theta}$ was used:

$$\begin{aligned} \hat{\Theta} \mathbf{E}(\mathbf{r}) &= \hat{T}_d^{-1} \hat{\Theta} \hat{T}_d \mathbf{E}(\mathbf{r}) \\ \hat{\Theta} &= \hat{T}_d^{-1} \hat{\Theta} \hat{T}_d \end{aligned}$$

Whenever that happens with operators, we can write it in the form:

$$\hat{T}_d \hat{\Theta} - \hat{\Theta} \hat{T}_d = 0$$

and bring the definition of **commutator** between two operators as in Quantum Mechanics:

$$[\hat{A}, \hat{B}] \triangleq \hat{A}\hat{B} - \hat{B}\hat{A} \quad (3.34)$$

If $[\hat{A}, \hat{B}] = 0$ we say that $\hat{\Theta}$ commutes with \hat{T}_d , and that implies that there are wavefunctions common to both. This is useful because sometimes eigenvalues and eigenfunctions of simple symmetry operators are easier to determine than those of $\hat{\Theta}$. The set of symmetry operators that commute with $\hat{\Theta}$ forms the symmetry group of the problem.

The fact that plane wave solutions are a solution of the problem is a consequence of them being solution to a symmetry operation that commutes with the operator of the problem. "When one has commuting operators, one can choose simultaneous eigenvectors of both operators" [13]

The shared eigenfunctions transform as irreducible representations of the symmetry group. Examples of operators that belong to the symmetry group of a given crystal lattice are Translation (both continuous and discrete), Rotation, and mirror operations.

Bloch-Floquet theory results from the special case of discrete translation operators. Also from quantum mechanics we can import the concept of commuting and commutators between operators.

3.4.3 Conservation of energy for waves in source less media

We define the energy of a field \mathbf{w} as its norm $\|\mathbf{w}\|^2 = (\mathbf{w}, \mathbf{w})$. Conservation of energy in time in a source less problem like that of equation 3.15 is obtained when $\|\mathbf{w}\|^2$ variation in time is zero, thus:

$$\frac{\partial \|\mathbf{w}\|^2}{\partial t} = \frac{\partial (\mathbf{w}, \mathbf{w})}{\partial t} = (\dot{\mathbf{w}}, \mathbf{w}) - (\mathbf{w}, \dot{\mathbf{w}}) = (\hat{\Theta}\mathbf{w}, \mathbf{w}) + (\mathbf{w}, \hat{\Theta}\mathbf{w}) = (\hat{\Theta}\mathbf{w}, \mathbf{w}) - (\hat{\Theta}\mathbf{w}, \mathbf{w}) = 0 \quad (3.35)$$

Remembering that in a problem that is not harmonic we have $\hat{\Theta}\mathbf{E} = \frac{\partial^2 \mathbf{E}}{\partial t^2}$ This means that under Hermitic operators such as $\hat{\Theta}$ the energy of the field is conserved

3.4.4 Energy functional of electromagnetic waves

By means of the **electromagnetic variational theorem** we can formulate an energy functional to be minimized. This functional is defined as a normalized inner product between the function

and the function multiplied by the operator ^{c1}:

$$U_f(\mathbf{E}) \triangleq \frac{(\mathbf{E}, \hat{\Theta}\mathbf{E})}{(\mathbf{E}, \mathbf{E})} \quad (3.36)$$

It is similar to other formulations used in fields like Quantum Mechanics and Classical mechanics such as expectation values, and energy Lagrangians. The process of finding solutions that minimize such a potential is the core of what methods like Galerkin do for solving differential equations. In chapter 4 we will use a similar expression in order to solve the wave equation using Galerkin with Finite Elements.

^{c1} NGZ: Este funcional se conoce como el cociente de Rayleigh.

Chapter 4

Finite element method

El calculo variacional es una disciplina que se encarga de encontrar el minimo de un funcional. En donde un funcional es el mapeo de un espacio vectorial a los reales. Si esta es la ecuacion diferencial

$$Lu = f$$

Entonces el residuo es

$$R(v) = Lv - f$$

y si se evalua en la solucion u

$$R(u) = 0$$

entonces minimizar un residio no tiene gracia, porque se trata de encontrar la solucion exacta a la ecuacion diferencial. Que es lo que no sabemos hacer. Pero entonces podemos proponer minimizar un residuo promediado, p. ej., la norma del error. Entonces definimos un residuo ponderado

$$Rp(u,v) = \int(v^*Lu - v^*f)$$

(weigthin se dice ponderar en espanhol). Entonces, uno propone una solucion con una forma conocida: senos y cosenos, polinomios, Gaussianas... Y encuentra la combinacion lineal de esas funciones que minimiza Rp (Ya estamos hablando de metodos aproximados para resolver la ecuacion diferencial).

The Finite Element Method approximate an integral formulation that is –in some sense– equivalent with a differential equation. This integral (weak) formulation could be obtained from a variational principle, such as the Principle of Virtual Works, or the Integral of Action [9], but could also be obtained from a more general approach like the Weighthed Residue Method [34, 22]. In the cas of electromagnetic waves, we can formulate a variational principle where the functional to be minimized is the energy carried by the electric and magnetic fields note[NGZ]Falta esta referencia, que ya se mencionó en el capitulo anterior.

This project uses the Galerkin Finite Element Method to construct an approximate solution of initial-boundary value problems involving the wave equation of electromagnetic fields [3.30](#).

Galerkin's method converts a continuous operator problem like a differential equation to a discrete problem by stating it as a weighted residual formulation.

4.1 Weak formulation of the problem

c1

In a weighted residual formulation weight functions are used in order to minimize a functional that is stated as the integral of the operator problem over the simulation domain [4.1](#).

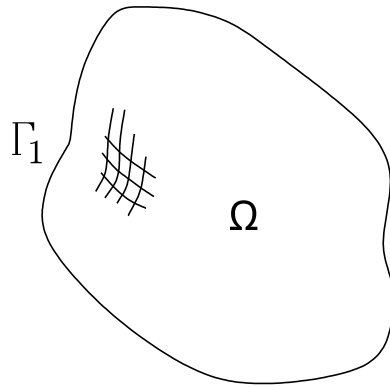


Figure 4.1: Abstract simulation domain and boundary

Galerkin method involves weight functions that belong to the same space as the solution. integration over the domain:

My weight functions wanna be called \mathbf{W} instead. They will belong to the same function space as \mathbf{E} .

$\int_{\Omega} \mathbf{W} \cdot (3.30)$:

$$\int_{\Omega} \mathbf{W} \cdot [\nabla \times (\bar{\mu}_r^{-1} \nabla \times \mathbf{E}) - k_0^2 \bar{\epsilon}_r \cdot \mathbf{E}] = -ik_0 Z_0 \int_{\Omega} \mathbf{W} \cdot \mathbf{J} \quad (4.1)$$

$$\int_{\Omega} \mathbf{W} \cdot \nabla \times (\bar{\mu}_r^{-1} \nabla \times \mathbf{E}) - k_0^2 \int_{\Omega} \mathbf{W} \cdot \bar{\epsilon}_r \cdot \mathbf{E} = -ik_0 Z_0 \int_{\Omega} \mathbf{W} \cdot \mathbf{J} \quad (4.2)$$

Now lets focus on the first integral on the left hand side of the equation. Here we will invoke the vector identity: $\mathbf{A} \cdot \nabla \times \mathbf{B} = \mathbf{B} \cdot \nabla \times \mathbf{A} - \nabla \cdot (\mathbf{A} \times \mathbf{B})$ Where $\mathbf{A} = \mathbf{W}$ and $\mathbf{B} = \bar{\epsilon}_r \nabla \times \mathbf{E}$ To express it as:

c1 NGZ: Hace falta una buena limpieza de estilo en este capítulo.

$$\int_{\Omega} \mathbf{W} \cdot \nabla \times (\bar{\mu}_r^{-1} \nabla \times \mathbf{E}) = \int_{\Omega} \bar{\mu}_r^{-1} \nabla \times \mathbf{E} \cdot \nabla \times \mathbf{W} - \int_{\Omega} \nabla \cdot (\mathbf{W} \times \bar{\mu}_r^{-1} \nabla \times \mathbf{E}) \quad (4.3)$$

The Divergence Theorem allows us to transform the volume integral on the second term of the right hand side to a closed surface integral:

$$\int_{\Omega} \nabla \cdot (\mathbf{W} \times \bar{\mu}_r^{-1} \nabla \times \mathbf{E}) = \oint_{\Gamma} \hat{n} \cdot (\mathbf{W} \times \bar{\mu}_r^{-1} \nabla \times \mathbf{E}) \quad (4.4)$$

And we will have two kinds of boundaries, Dirichlet and Newman (Reference some textbook), thus $\oint_{\Gamma} = \int_{\Gamma_D} + \int_{\Gamma_N}$. The Dirichlet contribution will be zero because the weight functions have also been chosen to be zero at Dirichlet boundaries ($\mathbf{W} |_{\Gamma_D} = 0$). One last step is to apply the triple product identity to the argument inside the Newman integral so that:

$$\hat{n} \cdot (\mathbf{W} \times \bar{\mu}_r^{-1} \nabla \times \mathbf{E}) = \mathbf{W} \cdot (\bar{\mu}_r^{-1} \nabla \times \mathbf{E} \times \hat{n}) = -\mathbf{W} \cdot (\hat{n} \times \bar{\mu}_r^{-1} \nabla \times \mathbf{E})$$

Substituting everything:

$$\int_{\Omega} \bar{\mu}_r^{-1} \nabla \times \mathbf{E} \cdot \nabla \times \mathbf{W} - k_0^2 \mathbf{W} \cdot \bar{\epsilon}_r \cdot \mathbf{E} + \int_{\Gamma_N} \mathbf{W} \cdot (\hat{n} \times \bar{\mu}_r^{-1} \nabla \times \mathbf{E}) = -ik_0 Z_0 \int_{\Omega} \mathbf{W} \cdot \mathbf{J} \quad (4.5)$$

4.2 Boundary conditions

Look for a nice reference that explain the situation on the boundaries and why is it important to define both the field at the boundary or the ratio of the field at the boundary. Maybe something related to the uniqueness of the solution. Pending to include.

$$\hat{n} \times \mathbf{E} = \mathbf{P} \quad \text{on } \Gamma_D \quad (4.6)$$

$$\hat{n} \times (\bar{\mu}_r^{-1} \nabla \times \mathbf{E}) = \mathbf{K}_N \quad \text{on } \Gamma_N \quad (4.7)$$

\mathbf{P} is the value for tangential electric field on Dirichlet boundaries Γ_D , η_r is the normalized surface impedance and \mathbf{K}_N is a function that represents boundary sources or electric field flux on Γ_N .

Replacing equation 4.7 in 4.5:

$$\begin{aligned} \int_{\Omega} \bar{\mu}_r^{-1} \nabla \times \mathbf{E} \cdot \nabla \times \mathbf{W} - k_0^2 \mathbf{W} \cdot \bar{\epsilon}_r \cdot \mathbf{E} &= -ik_0 Z_0 \int_{\Omega} \mathbf{W} \cdot \mathbf{J} \\ &\quad - \int_{\Gamma_N} \mathbf{W} \cdot \mathbf{K}_N \end{aligned} \quad (4.8)$$

$$\begin{aligned} \int_{\Omega} \bar{\mu}_r^{-1} \nabla \times \mathbf{E} \cdot \nabla \times \mathbf{W} - k_0^2 \mathbf{W} \cdot \bar{\epsilon}_r \cdot \mathbf{E} &= -ik_0 Z_0 \int_{\Omega} \mathbf{W} \cdot \mathbf{J} \\ &\quad - \int_{\Gamma_N} \mathbf{W} \cdot \mathbf{K}_N \end{aligned} \quad (4.9)$$

Using:

$$-\mathbf{W} \cdot (\hat{n} \times (\hat{n} \times \mathbf{E})) = (\hat{n} \times \mathbf{W}) \cdot (\hat{n} \times \mathbf{E})$$

4.3 Abstract form of the equation

Time to introduce bi linear operators. These operators are meant to ease mathematical manipulations. Let's do some definitions first: \mathbb{V} is a vector space of square integrable functions that vanishes at Dirichlet boundaries.

$$\mathbb{V} = \{v \in L^2(a, b) : a(v, v) < \infty \wedge v(\Gamma_D) = 0\}$$

$$L^2 = \left\{ v : \Omega \rightarrow \mathbb{R} \text{ such that } \int_{\Omega} v^2 d\Omega = 0 \right\}$$

$$\begin{aligned} a(\mathbf{W}, \mathbf{E}) &: \mathbb{V} \times \mathbb{V} \rightarrow \mathbb{R} \\ a(\mathbf{W}, \mathbf{E}) &= \int_{\Omega} \bar{\mu}_r^{-1} \nabla \times \mathbf{E} \cdot \nabla \times \mathbf{W} d\Omega \end{aligned} \quad (4.10)$$

$$\begin{aligned} m(\mathbf{W}, \mathbf{E}) &: \mathbb{V} \times \mathbb{V} \rightarrow \mathbb{R} \\ m(\mathbf{W}, \mathbf{E}) &= \int_{\Omega} k_0^2 \mathbf{W} \cdot \bar{\epsilon}_r \cdot \mathbf{E} d\Omega \end{aligned} \quad (4.11)$$

$$\begin{aligned} q(\mathbf{W}) &: \mathbb{V} \rightarrow \mathbb{R} \\ q(\mathbf{W}) &= \int_{\Gamma_N} \mathbf{W} \cdot \mathbf{K}_N \end{aligned} \quad (4.12)$$

$$\begin{aligned} f(\mathbf{W}) &: \mathbb{V} \rightarrow \mathbb{R} \\ f(\mathbf{W}) &= ik_0 Z_0 \int_{\Omega} \mathbf{W} \cdot \mathbf{J} \end{aligned} \quad (4.13)$$

Where \mathbf{J} and \mathbf{K}_N are known field and boundary conditions.

These operators take vectors as inputs and return scalars.

$$a(\mathbf{W}, \mathbf{E}) - m(\mathbf{W}, \mathbf{E}) = -f(\mathbf{W}) - q(\mathbf{W}) \quad (4.14)$$

4.4 Base functions and discretization

For 2D:

$$\mathbf{E} = E(x, y)_x \hat{a}_x + E(x, y)_y \hat{a}_y$$

The domain will be split in elements defined by relations between nodes (Add a figure and explain better how is it that you split a domain). The approximate solution will be computed using

interpolations applied to nodal values. Lets say that the set of nodes that represent values of the field in the domain is called η . On nodes belonging to Dirichlet boundaries we will know the value of the field and it is convenient to split the set of nodes into its known and unknown elements $\eta_D \cup \eta \setminus \eta_D = \eta$. Each physical node will contain two components of the field, one for x and the other for y . So the number of evaluation nodes gets doubled.

If N is the total number of values:

$$N = n_x + n_y$$

Where n_x and n_y are the number of evaluation nodes associated to fields in x and y . When programming it is convenient to distinguish where does a node belongs, so I will treat n_x and n_y as sets as well in order to build a notation for the sums based on how an iterator surfs a set.

$$n_x = n_x \in \eta_D + n_x \in \eta \setminus \eta_D$$

$$n_y = n_y \in \eta_D + n_y \in \eta \setminus \eta_D$$

If I say:

$$i : n_x \in \eta_D$$

That will mean that the iteration will occur on the indexes that belong to the set of nodes in the Dirichlet region associated to x component of the field.

$$\begin{aligned} E(x, y)_x &\approx \sum_{i: n_x \in \eta_D} h_i E_i^x + \sum_{i: n_x \in \eta \setminus \eta_D} h_i E_i^x \\ E(x, y)_y &\approx \sum_{i: n_y \in \eta_D} h_i E_i^y + \sum_{i: n_y \in \eta \setminus \eta_D} h_i E_i^y \end{aligned}$$

Left side is known values and right side is unknowns.

In the same way but without knowing W on the boundary:

$$\mathbf{W} = W(x, y)_x \hat{a}_x + W(x, y)_y \hat{a}_y$$

$$\begin{aligned} W(x, y)_x &\approx \sum_{i: n_x \in \eta_D} h_i W_i^x + \sum_{i: n_x \in \eta \setminus \eta_D} h_i W_i^x \\ W(x, y)_y &\approx \sum_{i: n_y \in \eta_D} h_i W_i^y + \sum_{i: n_y \in \eta \setminus \eta_D} h_i W_i^y \end{aligned}$$

I believe that with source terms and boundaries the expansion can be made either with only the known values on nodes, or with interpolation functions such as those before. Right here I think I will ommit interpolation of \mathbf{J} and \mathbf{K}_N .

$$\mathbf{J} = J(x, y)_x \hat{a}_x + J(x, y)_y \hat{a}_y$$

$$\begin{aligned} J(x, y)_x &\approx \sum_{i: n_x \in \eta_D} h_i J_i^x + \sum_{i: n_x \in \eta \setminus \eta_D} h_i J_i^x \\ J(x, y)_y &\approx \sum_{i: n_y \in \eta_D} J_i^y + \sum_{i: n_x \in \eta \setminus \eta_D} J_i^y \end{aligned}$$

$$\mathbf{K}_N = K(x, y)_x \hat{a}_x + K(x, y)_y \hat{a}_y$$

$$\begin{aligned} K(x, y)_x &\approx \sum_{i: n_x \in \eta_D} h_i K_i^x + \sum_{i: n_x \in \eta \setminus \eta_D} 0 \\ K(x, y)_y &\approx \sum_{i: n_y \in \eta_D} h_i K_i^y + \sum_{i: n_x \in \eta \setminus \eta_D} 0 \end{aligned}$$

Definition of h_i is left for later because its complicated.

Substitution of \mathbf{E} and \mathbf{W} , into ?? is a mess. To make it easier lets use the operators and their nice properties. To be bilinear is to be linear in both arguments, to be linear means to satisfy additivity and homogeneity. An illustration of this:

$$a(\alpha u + \beta v, w) = \alpha a(u, w) + \beta a(v, w)$$

$$a(u, \alpha v + \beta w) = \alpha a(u, v) + \beta a(u, w)$$

The rotational and dot product inside the integrals defined in the abstract forms are linear. A proof which I am pending to do will show that the operators themselves are bi linear. Also, it remains to be prooved if the following is true:

$$a(u, v) = a(v, u)$$

$$m(u, v) = m(v, u)$$

So the following can happen:

$$\begin{aligned}
a(W_x, E_x) &= a \left(\sum_{i: n_x \in \eta_D} h_i W_i^x, \sum_{j: n_x \in \eta_D} h_j E_j^x \right) + a \left(\sum_{i: n_x \in \eta \setminus \eta_D} h_i W_i^x, \sum_{j: n_x \in \eta \setminus \eta_D} h_j E_j^x \right) \\
&= \sum_{i: n_x \in \eta_D} W_i^x a \left(h_i, \sum_{j: n_x \in \eta_D} h_j E_j^x \right) + \sum_{i: n_x \in \eta \setminus \eta_D} W_i^x a \left(h_i, \sum_{j: n_x \in \eta \setminus \eta_D} h_j E_j^x \right) \\
&= \sum_{i: n_x \in \eta_D} W_i^x \sum_{j: n_x \in \eta_D} E_j^x a(h_i, h_j) + \sum_{i: n_x \in \eta \setminus \eta_D} W_i^x \sum_{j: n_x \in \eta \setminus \eta_D} E_j^x a(h_i, h_j) \\
&= \sum_{j: n_x \in \eta_D} a(h_i, h_j) E_j^x \sum_{i: n_x \in \eta_D} W_i^x + \sum_{j: n_x \in \eta \setminus \eta_D} a(h_i, h_j) E_j^x \sum_{i: n_x \in \eta \setminus \eta_D} W_i^x
\end{aligned} \tag{4.15}$$

$$\begin{aligned}
\sum_{j: n_x \in \eta_D} E_j^x &= \vec{g}_j^x \\
\sum_{i: n_x \in \eta \setminus \eta_D} W_i^x &= \vec{W}^x \\
\sum_{j: n_x \in \eta \setminus \eta_D} E_j^x &= \vec{E}^x \\
\vec{g}_i &= \vec{g}_j^x + \vec{g}_j^y \quad j = 1..N
\end{aligned}$$

\vec{g}_j is a vector of size N that holds values of E on each Dirichlet boundary node for both x , and y components. Vector \vec{g}_i^y follows from a similar procedure on E_y . It is of importance for me as the one to program to say that: even though the sets defined under the summation are subsets of the set of all nodes, when programming, their associate vectors will span the whole domain. In other words this notation stands for entries to indexes to vectors that may be defined full of zeroes. Or in a different approach: j in $j : n_x \in \eta_D$ can be indexes 1 and N meaning that the first and last nodes belong to Dirichlet boundary points on x . All other elements of the vector are undefined and hold their initiation value zero.

Changing the indexes i,j and using the definition of dot product in a matrix notation we can translate the abstract form as:

$$a(W_x, E_x) = \langle \mathbb{A} \vec{g}^x, \vec{W}^x \rangle + \langle \mathbb{A} \vec{E}^x, \vec{W}^x \rangle$$

Where \mathbb{A} is a matrix whose elements contain the indexed integration over the basis functions h_i , and h_j , these are known values because we know the form of the functions and can easily calculate the integrals by numerical or analytic means.

$$\mathbb{A} = \mathbb{A}^x + \mathbb{A}^y$$

$$\mathbb{A}^x = \sum_{i,j}^{n_x \in \eta \setminus \eta_D} a(h_i, h_j) + \sum_{i,j}^{n_y \in \eta \setminus \eta_D} a(h_i, h_j)$$

The product $\mathbb{A}^x \vec{g}^x = \vec{d}^x$ will be called the Dirichlet vector.

$$a(W_x, E_x) = \langle \vec{d}^x, \vec{W}^x \rangle + \langle \mathbb{A}^x \vec{E}^x, \vec{W}^x \rangle \quad (4.16)$$

In a very similar way but now substituting the approximate functions into the kinetic operator $m(\mathbf{W}, \mathbf{E})$ we get:

$$\begin{aligned} m(W_x, E_x) &= \langle \mathbb{M}^x \vec{g}^x, \vec{W}^x \rangle + \langle \mathbb{M}^x \vec{E}^x, \vec{W}^x \rangle \\ m(W_x, E_x) &= \langle \vec{b}^x, \vec{W}^x \rangle + \langle \mathbb{M}^x \vec{E}^x, \vec{W}^x \rangle \end{aligned} \quad (4.17)$$

With:

$$\begin{aligned} \mathbb{M} &= \mathbb{M}^x + \mathbb{M}^y \\ \mathbb{M} &= \sum_{i,j}^{n_x \in \eta \setminus \eta_D} m(h_i, h_j) + \sum_{i,j}^{n_y \in \eta \setminus \eta_D} m(h_i, h_j) \end{aligned}$$

And the same follows with operators q and f :

$$f(W_x) = \langle \vec{f}^x, \vec{W}^x \rangle \quad (4.18)$$

$$q(W_x) = \langle \vec{q}^x, \vec{W}^x \rangle \quad (4.19)$$

$$\begin{aligned} \vec{f}_i^x &= ik_0 Z_0 \sum_{i: n_x \in \eta} \int_{\Omega} h_i J_i^x \\ \vec{q}_i^x &= \sum_{i: n_x \in \eta_N} \int_{\Gamma_N} h_i K_i^x \end{aligned}$$

Where I introduced a subset of the set $\eta \setminus \eta_D$ called η_N which represents nodes on Newman boundaries.

Substituting definitions: 4.16, 4.17, 4.19, 4.18 in equation 4.14, we get:

$$\begin{aligned} \langle \vec{d}^x, \vec{W}^x \rangle + \langle \mathbb{A}^x \vec{E}^x, \vec{W}^x \rangle - \langle \vec{b}^x, \vec{W}^x \rangle - \langle \mathbb{M}^x \vec{E}^x, \vec{W}^x \rangle &= -\langle \vec{f}^x, \vec{W}^x \rangle - \langle \vec{q}^x, \vec{W}^x \rangle \\ \langle \mathbb{A}^x \vec{E}^x - \mathbb{M}^x \vec{E}^x, \vec{W}^x \rangle &= \langle \vec{b}^x - \vec{d}^x - \vec{q}^x - \vec{f}^x, \vec{W}^x \rangle \end{aligned} \quad (4.20)$$

Being \vec{W}^x an arbitrary function, the following linear system of equations appear:

$$(\mathbb{A}^x - \mathbb{M}^x) \vec{E}^x = \vec{b}^x - \vec{d}^x - \vec{q}^x - \vec{f}^x \quad (4.21)$$

Similarly and following exactly the same procedure:

$$(\mathbb{A}^y - \mathbb{M}^y) \vec{E}^y = \vec{b}^y - \vec{d}^y - \vec{q}^y - \vec{f}^y \quad (4.22)$$

And right now I guess those can be summed. I really don't get why I chose to separate them in the first place. Guess it was in order to make it clear that the components where independent.

So, Matrices and vectors are of the same size (N) for both equations, and the places where one has zeros has values in the other. I don't see any impediment to sum 4.21 and 4.22:

$$(\mathbb{A}^x - \mathbb{M}^x) \vec{E}^x + (\mathbb{A}^y - \mathbb{M}^y) \vec{E}^y = \vec{b} - \vec{d} - \vec{q} - \vec{f}$$

A system that I really don't know if can be brought to the form

$$\mathbb{K} \vec{E} = \vec{v}$$

Something that I've seen happening in many books is to remove rows and columns associated to Dirichlet positions of E in the matrices and vectors of the equation. This is done because we already know the values of E for those points and their information is already saved in vector \vec{d} . I will add the symbol $\backslash D$ before the symbols to note that Dirichlet rows and columns should be deleted.

$$\backslash D \left[(\mathbb{A}^x - \mathbb{M}^x) \vec{E}^x + (\mathbb{A}^y - \mathbb{M}^y) \vec{E}^y = \vec{b} - \vec{d} - \vec{q} - \vec{f} \right]$$

4.5 Vectorial vs scalar formulation

4.6 Edge elements vs Node Elements

4.7 Second order elements, shape functions.

4.8 Numerical integration and Gauss quadrature

4.9 Mass matrices

i What is the meaning of Mass matrices in EM?

discrete representation of a continuous distribution of something that multiplies the second time derivative of the field.

Mass matrices are cataloged as consistent or diagonal. Consistent mass matrices use the same shape functions as the ones used to generate the element stiffness matrix. All reference to mass matrices mentioned before, were consistent. [23] The other way to formulate mass matrices is the lumped mass matrix. Which is made by avoiding the interpolation and simply placing particle masses m_i at nodes i of an element such that $\sum m_i$ is the total element mass.

The great advantage of lumped mass matrices is that they are diagonal and the solution of the system of equations can be performed in a explicit manner convenient for big computational domains. However, precision is lost by not stating mass as functions to be interpolated.

To form a lumped mass matrix one can use the HRZ Lumping scheme which consist on the following algorithm [23]:

1. Compute the diagonal coefficients of the consistent mass matrix.
2. Compute the mass for each element m .
3. Compute the trace of the matrix s .
4. scale all the diagonal coefficients by multiplying them by the ratio $\frac{m}{s}$.

4.10 Explicit formulation

central-difference method Aproximates the second order derivative of \mathbf{E} by expanding \mathbf{E}_{n+1} and \mathbf{E}_{n-1} in taylor series about time $n \Delta t$:

$$\mathbf{E}_{n+1} = \mathbf{E}_n + \delta t \dot{\mathbf{E}}_n + \frac{\delta t^2}{2} \ddot{\mathbf{E}}_n + \frac{\delta t^3}{6} \dddot{\mathbf{E}}_n + O(\delta t^4) \quad (4.23)$$

$$\mathbf{E}_{n-1} = \mathbf{E}_n - \delta t \dot{\mathbf{E}}_n + \frac{\delta t^2}{2} \ddot{\mathbf{E}}_n - \frac{\delta t^3}{6} \dddot{\mathbf{E}}_n + O(\delta t^4) \quad (4.24)$$

Restricting to fourth-order accuracy ($O(\delta t^4)$) and adding 4.23 to 4.24 one can easily solve for \mathbf{E}_{n+1} :

$$\ddot{\mathbf{E}}_n = \frac{1}{\delta t^2} (\mathbf{E}_{n+1} - 2\mathbf{E}_n + \mathbf{E}_{n-1}) \quad (4.25)$$

subscript n denotes time $n\delta t$ with δt being the selected timestep.

Replacing into our general formulation one gets (fix details):

$$\frac{1}{\delta t^2} \mathbb{M} \mathbf{E}_{n+1} = \frac{1}{\delta t^2} \mathbb{M} [2\mathbf{E}_n - \mathbf{E}_{n-1}] \mathbb{A} \mathbf{E}_n \quad (4.26)$$

Nice concluding remarks in page 424 of the book.

Chapter 5

Implementation

5.1 Object Oriented Paradigm

5.2 Classes, Diagrams and flow charts of PeYeQM

Chapter 6

Results

As mentioned in the introduction, a software platform able to simulate propagation of electromagnetic waves in photonic crystals was developed. In chapter 3 the equations that rule the problem where stated, and background behind one method of solution for them using FEA has been discussed in chapter 4. In this chapter the solutions obtained by applying these concepts are presented and compared with either their analytic solutions or numerical solutions from the literature.

6.1 Electrostatic benchmark tests

Now, platform PeyeQM was built in a [bottom-up](#) process that started by making a FE solver that could handle static scalar problems of electron confinement in 2D potential wells for application in Quantum Mechanics. This project involved an upgrade of that platform that began with the implementation of support for vector formulations, and a transition to Object Oriented Paradigm that could improve flexibility and maintenance.

The first section of this chapter shows the results obtained for Electrostatic benchmark tests, and were made in order to assert the accuracy of the static vectorial solver, and routines for the construction of stiffness matrices.

6.1.1 Electric field due to charged elements

Parallel plate capacitor

The first experiment was to simulate the most basic field we could think of, this is, that inside a parallel plate capacitor, where field lines go straight from one plate to the other.

Electric fields satisfy equation 3.5. If there are no sources or sinks ($-\frac{\partial \mathbf{B}}{\partial t} = 0$), then the field \mathbf{E} is said to be *irrotational* and by an identity of vector calculus we know that there must exist a scalar field V whose gradient is a valid Electrostatic vector field:

$$\nabla \times \nabla V = 0 \quad (6.1)$$

Scalar equations are easier to solve and are very useful when the medium is homogeneous and isotropic, this is the reason why many books stick with scalar problems and leave the process of obtaining \mathbf{E} as performing on V the derivations in operator ∇ . Using the scalar potential as an intermediate step for the solution of \mathbf{E} stops being a good idea when interfaces between mediums and sharp geometries appear, and a direct solution using vector fields gains relevance.

In a parallel plate capacitor like that in figure 6.1, we consider two (infinite, parallel, plane, perfectly conducting, charged) plates that occupy the planes $x = 0$ and $x = d$ kept at potentials $V = 0$ and $V = V_0$ respectively. With plates of very large dimensions compared to the spacing between them, the potential becomes a function of x only, and equation 6.1 becomes:

$$\frac{d^2V}{dx^2} = 0$$

Integrating twice, we get:

$$V(x) = Ax + B \quad (6.2)$$

Where A and B are constants of integration solved by using boundary conditions.

$$V(0) = A0 + B = 0 \quad \text{or} \quad B = 0$$

$$V(d) = Ad + B = V_0 \quad \text{or} \quad A = \frac{V_0}{d}$$

Making the particular solution for the potential:

$$V = \frac{V_0}{d}x \quad \text{for } 0 < x < d$$

The field is then obtained by taking the gradient of V , and we add a $-$ sign taking into account that \mathbf{E} is a conservative field.

$$\mathbf{E} = -\nabla V = -\frac{dV}{dx}\hat{a}_x = -\frac{V}{d}\hat{a}_x \quad (6.3)$$

This means that the field is uniform and directed from the higher potential plate to the lower potential plate as shown in 6.1 ??.

A rectangular region was meshed and Dirichlet boundary condition were applied in the bottom and top plates as a field pointing down. Separation d is taken unitary and the result is shown in figure 6.2.

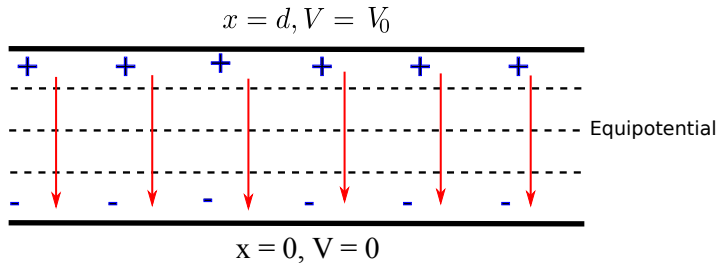


Figure 6.1: Cross sectional view of parallel plate capacitor.

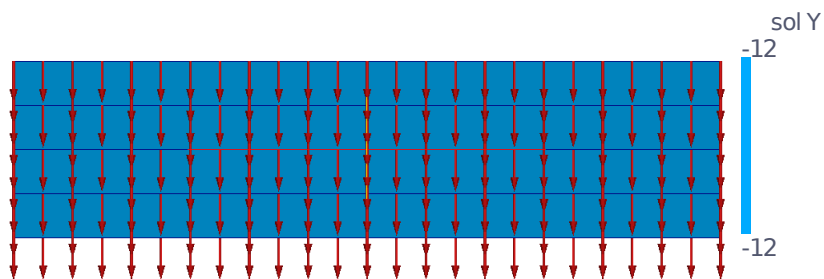


Figure 6.2: Solution of electric field in parallel plate capacitor.

It can be seen that the lines don't change in either magnitude or direction, and go from the charged plate with potential V_0 to the bottom plate as expected.

This test showed that the routines for assembling stiffness matrices are capable of continuing a simple field over a distance between two boundaries.

The script for producing this simulation and the necessary input files can be seen in the *repository*.

Charged cylinder

The next field problem to solve in order to test PeyeQM was one with circular geometry. The solution for the field due to a point charge or a charged cylinder was used to compare the precision of the method for representing fields with two components.

Gauss law 3.3 in spherical coordinates, assuming a homogeneous medium with scalar permittivity is:

$$\epsilon \int_S \mathbf{E} \cdot d\mathbf{S} = \int_V \rho dV \quad (6.4)$$

Where $\int_V \rho dV = q$ is the charge of the particle. If that charge is distributed uniformly, then there are no preferred directions and the electric field must be radial [5] and have constant intensity over

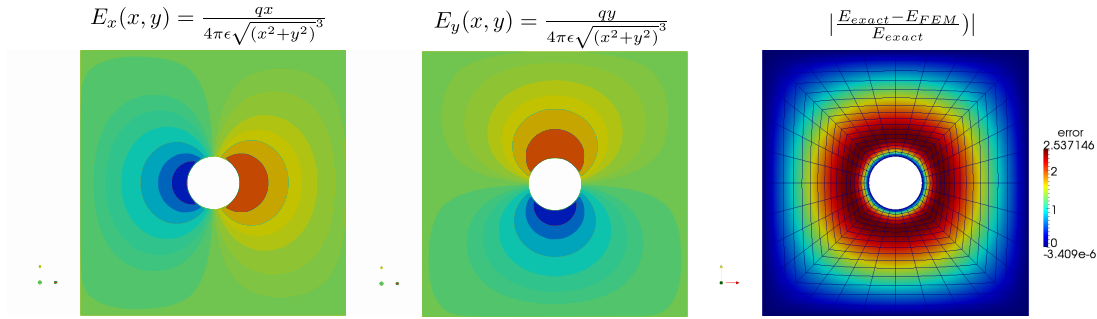


Figure 6.3: Whole simulation of Electric field due to a charged cylinder. Left, Numerical result for the x component of the field. Middle, x component of the solution, and, right, mesh and error calculated between analytic formula and results.

spherical shells. So for an arbitrary spherical shell of radius r :

$$\epsilon \mathbf{E} \int_\theta \int_\phi r^2 \sin(\theta) d\phi = q$$

$$\mathbf{E}_r(r) = \frac{q}{4\pi\epsilon r^2} \hat{r}$$

Now, this has to be transformed into Cartesian coordinates in order to input boundary conditions. If we consider r as the magnitude of vector \vec{r} in the unitary direction \hat{r} then we can transform it to a linear combination of unitary vectors \hat{x} and \hat{y} by the following:

$$\vec{r} = r \cos(\theta) \hat{x} + r \sin(\theta) \hat{y} \quad (6.5)$$

And by trigonometry we know that $\cos(\theta) = \frac{x}{r}$ and $\sin(\theta) = \frac{y}{r}$. Making the necessary substitutions we get to:

$$\mathbf{E}_r(r) = \mathbf{E}_x(x, y) + \mathbf{E}_y(x, y) = \frac{qx}{4\pi\epsilon\sqrt{(x^2 + y^2)^3}} \hat{x} + \frac{qy}{4\pi\epsilon\sqrt{(x^2 + y^2)^3}} \hat{y} \quad (6.6)$$

So, a plot the solution after simulating should match a representation of this analytic result. We initially proposed a model where the charged cylinder or point source is modeled as a whole circle inside a square domain, the results of the simulation (figure 6.3) showed that for this kind of problem where the field decays in the form $\frac{1}{r^2}$ it was better to use finer meshes and take advantage of symmetries to reduce the computational cost. Taking just an eighth of the model, and reshaping the outer boundary to a circle improved the quality of the elements and allowed us to use a finer mesh. figure 6.4 shows the y and x components of the field as well as the error between the simulation and the analytic solution. For the simulation factor $\frac{q}{2\pi\epsilon}$ has been normalized to 1, and the mesh was done using 1996 QUAD8 elements with 5525 nodes, thus 11050 degrees of freedom. As a comparison, the simulation of the whole circle involved 2432 elements and 7040 nodes with 14080 degrees of freedom, but it solved for a domain that was eight times bigger.

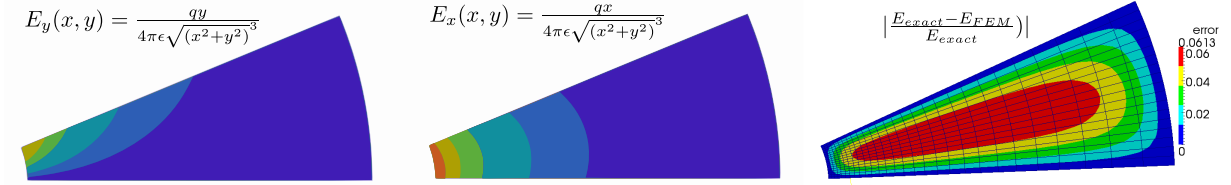


Figure 6.4: Segment of the simulation for Electric field due to a charged cylinder. a) Numerical result for the y component of the field, b) x component of the solution, c) Mesh and error calculated between analytic formula and results.

Electric Dipole, two charged spheres.

A similar simulation was performed using two semicircular surfaces, taking advantage of inversion symmetry along x axis. Boundary conditions are Dirichlet conditions over the circles and the rectangular boundaries on top, and Neumann conditions set to 0 on bottom lines. The analytic solution is simply the overlapping of the field due to charge 1 and charge 2, having one of them centered in the origin, and the other displaced by a distance d . The field everywhere can be expressed as:

$$\mathbf{E}_1(x, y) = x(x^2 + y^2)^{-\frac{3}{2}} \hat{x} + y(x^2 + y^2)^{\frac{3}{2}} \hat{y} \quad (6.7)$$

$$\mathbf{E}_2(x, y) = -(x-4)((x-4)^2 + y^2)^{-\frac{3}{2}} \hat{x} - y((x-4)^2 + y^2)^{\frac{3}{2}} \hat{y} \quad (6.8)$$

$$\mathbf{E}_x = \left[x(x^2 + y^2)^{-\frac{3}{2}} - (x-4)((x-4)^2 + y^2)^{-\frac{3}{2}} \right] \hat{x} \quad (6.9)$$

$$\mathbf{E}_y = \left[y(x^2 + y^2)^{\frac{3}{2}} - y((x-4)^2 + y^2)^{\frac{3}{2}} \right] \hat{y} \quad (6.10)$$

Where again $\frac{q}{2\pi\epsilon} = 1$ for the left charged circle and -1 for the one on the right at a distance $d = 4$. Figure 6.5 shows components x and y of the resulting field as obtained from the FE solver. The direction of the field lines can be observed by means of arrow glyphs in figure 6.6, where field lines go outwards in the positively charged cylinder and inwards in the negative. In the same way as before, a comparison between analytic and numerical solutions was performed (figure 6.7) and error appeared to be magnified in the region between cylinders. This value keeps being higher than expected, and different meshing schemes were tested in order to improve accuracy. Less error was observed using adaptative meshing methods than structured grids. The current mesh for this simulation has 510 elements and 1622 degrees of freedom, a future simulation is proposed with finer meshes using a PC with bigger RAM.

$$\mathbf{E}_x = \left[x (x^2 + y^2)^{-\frac{3}{2}} - (x - 4) ((x - 4)^2 + y^2)^{-\frac{3}{2}} \right] \quad \mathbf{E}_y = \left[y (x^2 + y^2)^{\frac{3}{2}} - y ((x - 4)^2 + y^2)^{\frac{3}{2}} \right]$$

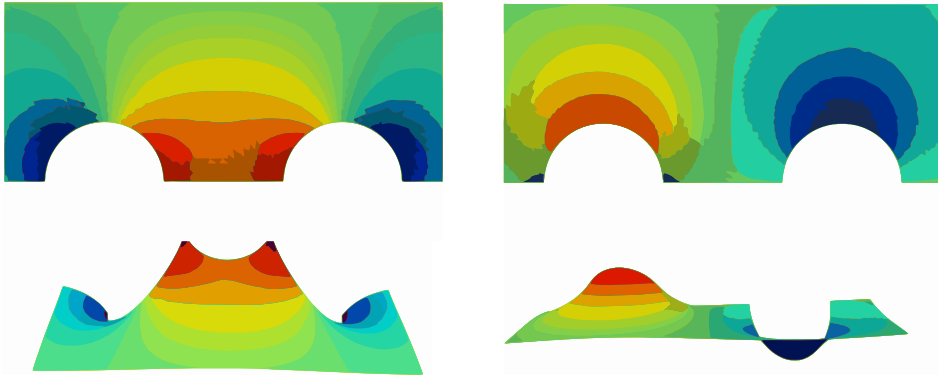


Figure 6.5: Components of the electric field after simulating a problem of two cylinders with opposite charges.

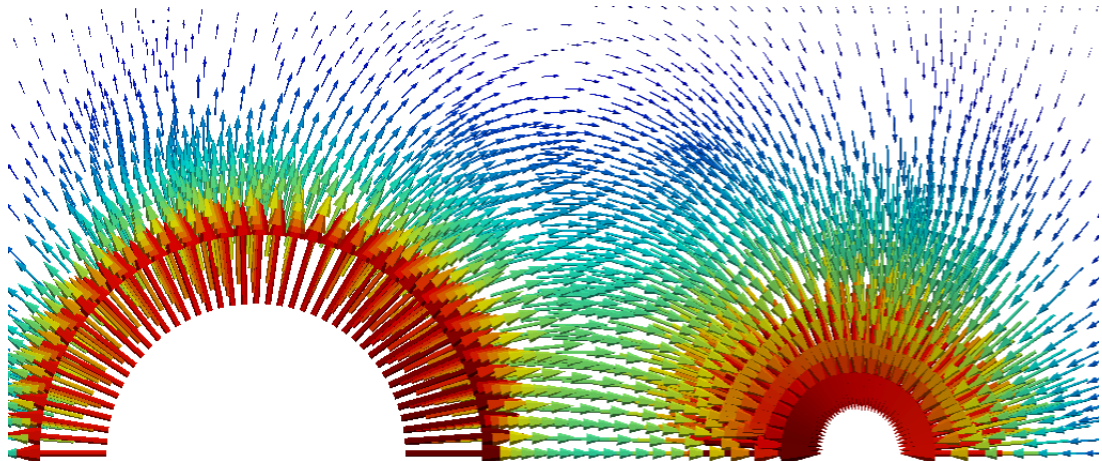


Figure 6.6: Arrow glyphs of the solution for the dipole problem. Length and color of the arrow indicate magnitude of the field. As expected, the field points from the positively charged cylinder to the negative.

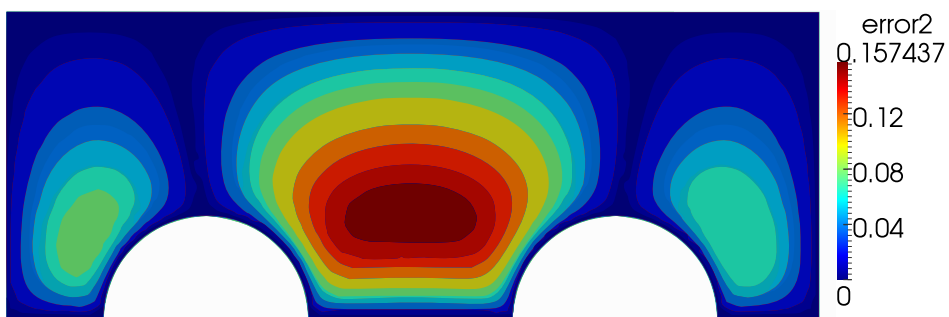


Figure 6.7: Error calculation of simulation against exact solution. The method reproduces the nature of the problem, but a finer mesh is needed to obtain precise results.

6.2 Harmonic benchmark tests

The second section regards solutions of eigenvalue problems, either for closed domains or infinite and periodic ones. The first part will deal with simulation of resonant modes in wave guides, and the second with free waves and periodic crystals. In this stage of PeyeQM we knew that the program was capable of assembling stiffness matrices and solving systems of linear equations, what the following tests with waveguides would give was the certainty that we were able to form mass matrices as well as solve the eigenvalue problems associated with a formulation of the form:

$$\mathbf{A}\tilde{\mathbf{E}} = \mathbf{M}\tilde{\mathbf{E}}$$

6.2.1 Eigenvalues and modes in waveguides

Ideal wave guides can be modeled by a source-less version of the wave equation for time harmonic fields 3.21 in arbitrary 2D domains closed by a metallic boundary that guarantees Dirichlet condition $\mathbf{E} = 0$ at Γ . This problem is relevant in electromagnetism and telecommunications because it is the principle behind many applications such as data transmission in fiber optics, and microwaves. Here, the 2D domain represents a cross section of a metallic structure that guides waves along its axis. We are particularly interested in knowing two things:

1. The modes or wave functions that are solution to the equation for a particular shape.
2. The frequencies associated to those modes or shapes.

And will start by introducing the analytic solution behind simple wave guides such as rectangular and circular guides.

Rectangular waveguides

In transverse magnetic fields (TM) that travel inside a waveguide whose axis is over z , we have $\mathbf{H}_z = 0$ and solve for \mathbf{E} components. Solutions of equation 3.30 where the medium inside the wave guide is a perfect dielectric, and for eigenvalues $\vec{k}^2 = \omega^2\mu\epsilon$ is a lengthy but straightforward process that involves separation of variables and use of boundary conditions:

$$\mathbf{E}_x = 0 \quad \text{for } y = 0, 0 < x < a \tag{6.11}$$

$$\mathbf{E}_x = 0 \quad \text{for } y = b, 0 < x < a \tag{6.12}$$

$$\mathbf{E}_y = 0 \quad \text{for } x = 0, 0 < y < b \tag{6.13}$$

$$\mathbf{E}_y = 0 \quad \text{for } x = a, 0 < y < b \tag{6.14}$$

A description of the solution process is left for the reader to look up in references such as Rao [21] or Jianming [12]. What is found in the process is that only certain discrete frequencies are allowed inside the waveguide, and they are given by:

$$\omega_{n,m} = \frac{1}{\sqrt{\mu\epsilon}} \sqrt{\left(\frac{m\pi}{a}\right)^2 + \left(\frac{n\pi}{b}\right)^2} \quad m, n = 0, 1, 2, \dots \quad (m = n \neq 0) \quad (6.15)$$

Where ω is indexed by integers n, m and the trivial solution $\omega = 0$ is excluded. a is the width of the rectangular cross section and b is its height. The wave functions that are solution to this eigenproblem for each component of the field are in the following general form:

$$\mathbf{E}_z = A \sin \frac{m\pi x}{a} \sin \frac{n\pi x}{b} e^{\mp jk_z z} \quad (6.16)$$

$$\mathbf{E}_x = \mp jB \frac{m\pi}{a} \cos \frac{m\pi x}{a} \sin \frac{n\pi x}{b} e^{\mp jk_z z} \quad (6.17)$$

$$\mathbf{E}_y = \mp jC \frac{n\pi}{b} \sin \frac{m\pi x}{a} \cos \frac{n\pi x}{b} e^{\mp jk_z z} \quad (6.18)$$

For our comparisons we will only look at how closely the shapes of the simulated solution represent \mathbf{E} in 6.16, and how similar are the analytic and numeric natural frequencies of the guide ω .

The numerical solution for rectangular waveguide has less degenerate modes, and the shapes look better.

| Comparison of ω^2 for square wave-guide | | | | |
|--|------------|-------------|-------------|-------------|
| m,n | 1,1 | 1,2 | 2,2 | 3,1 |
| FEM | 4.93480857 | 12.33721117 | 19.73961759 | 24.6763011 |
| Anlytic | 4.93480220 | 12.33700550 | 19.73920880 | 24.67401100 |

| Comparison of ω^2 for rectangular waveguide $a = 2b$ | | | | |
|---|------------|------------|-----------|-------------|
| m,n | 1,1 | 2,1 | 3,1 | 1,2 |
| FEM | 3.08425459 | 4.93480795 | 8.0190859 | 12.33717191 |
| Anlytic | 3.08425137 | 4.93480220 | 8.0190535 | 12.33700550 |

Circular waveguides

For a circular wave guide the modes are

| Comparison of $\frac{\omega}{a}$ for circular wave-guide | | | | |
|--|------------|------------|------------|------------|
| m,n | 0,1 | 1,1 | 2,1 | 0,2 |
| FEM | 2.40482634 | 3.83171343 | 5.13564189 | 5.52012378 |
| Anlytic | 2.40482555 | 3.83170597 | 5.13562230 | 5.52007811 |

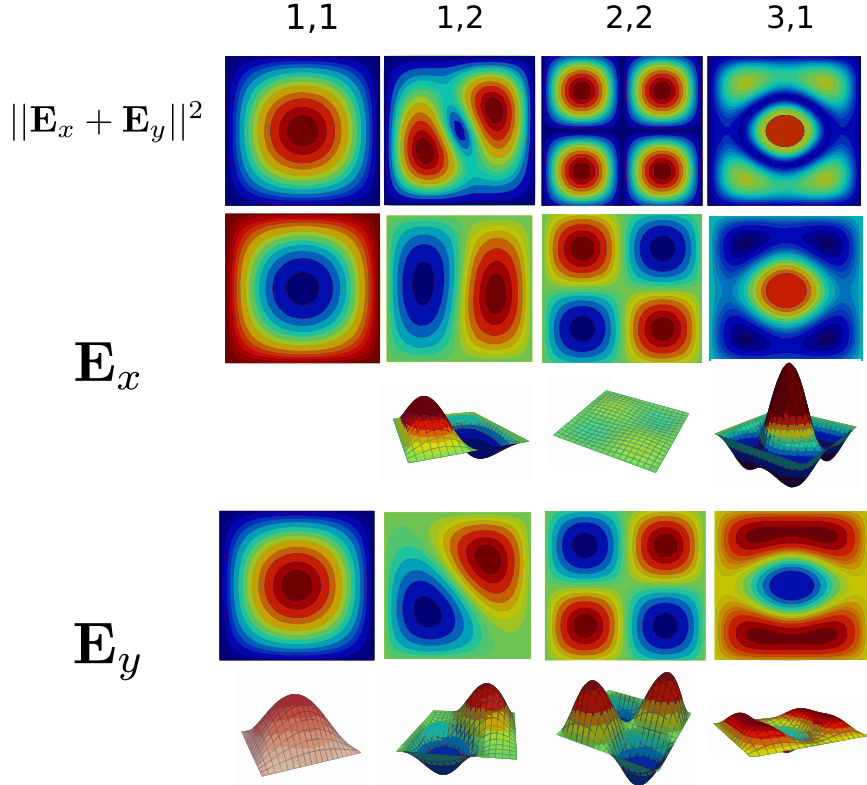


Figure 6.8: Results for three different modes from the simulation of a square shaped waveguide with side $a = b = 2$

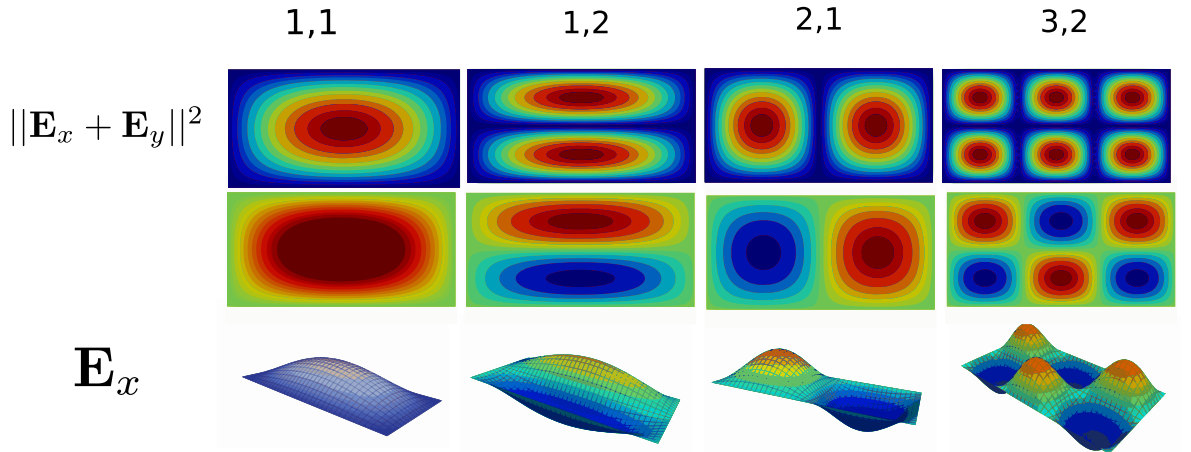


Figure 6.9: Results for three different modes from the simulation of a rectangle shaped waveguide with sides $a = 4$ and $b = 2$.

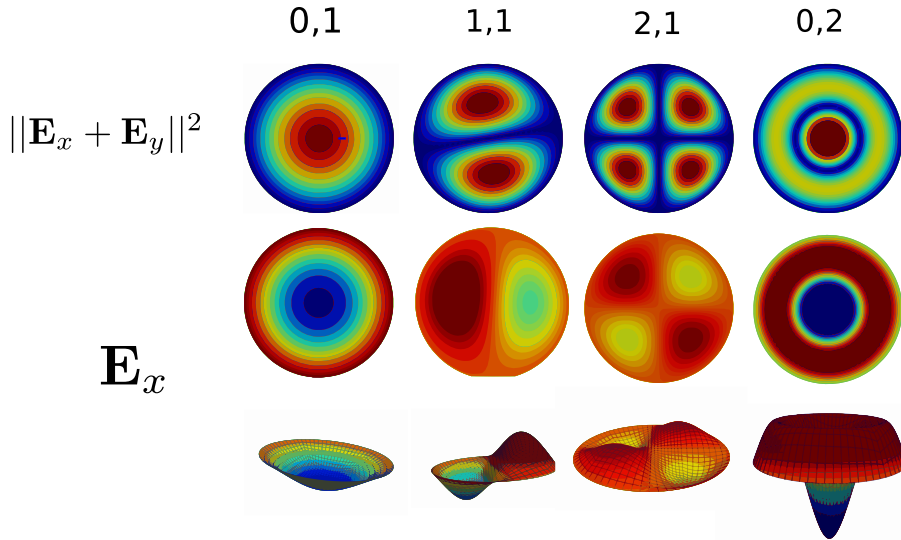


Figure 6.10: Results for three different modes from the simulation of circular waveguide with radius $a = 2$.

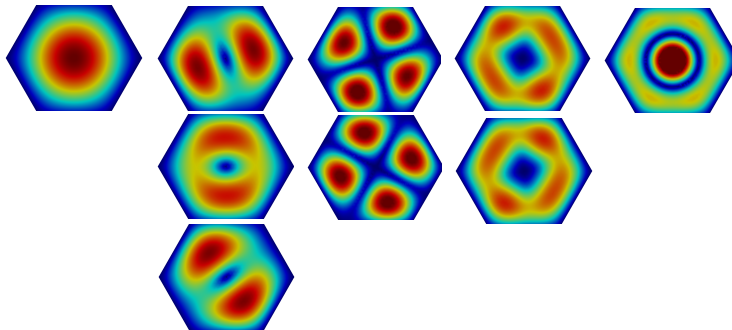


Figure 6.11: Degeneracy of modes from the simulation of hexagonal waveguide.

Hexagonal waveguide

Threefold degeneracy is seen in modes of hexagonal guides due to symmetries.

| Comparison of ω^2 for hexagonal wave-guide | | | | |
|---|------------|------------|-------------|------------|
| m,n | 0,1 | 1,1 | 2,1 | 0,2 |
| FEM | 5.34990939 | 8.51630317 | 11.39340788 | 12.2461672 |
| Anlytic | | | | |

Elliptical waveguide

The closest to a reference from which to compare the solutions of elliptical waveguides was a study of oscillationin an elliptic membrane by J. Gutiérrez Vega [11]. Shapes shown in figure 6.12 are in

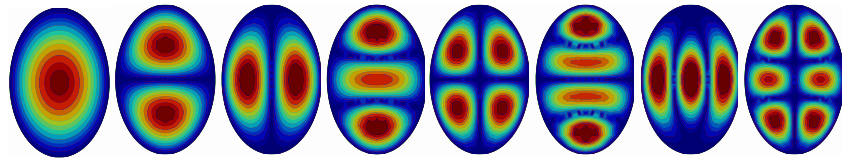


Figure 6.12: Results for the first 8 modes from the simulation of an elliptical waveguide with minor axis $a = 2$ and major axis $b = 3$.

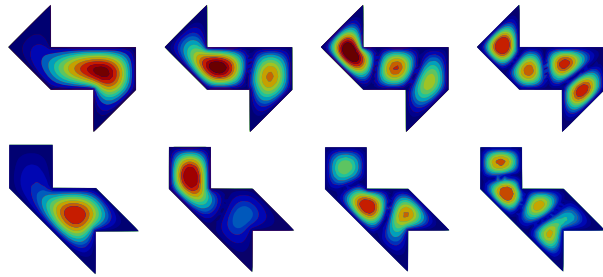


Figure 6.13: First 4 modes from the simulation of two isospectral shapes as taken from [4].

agreement with the images in the reference.

| First four frequencies ω for hexagonal wave-guide | | | | |
|--|--------|--------|--------|--------|
| FEM | 2.0195 | 2.4149 | 2.6627 | 2.9457 |

Isoespectral shapes

Tested the solver by performing the computation of isospectral shapes as proposed by Chapman in [4]. The idea behind this was to obtain the same eigenvalues from different shapes by taking advantage of possible mappings between figures that share certain properties. A comparison between eigenvalues is presented in table 6.2.1, and the first 4 non-degenerate modes are shown in figure 6.13.

| Comparison of ω^2 for two isospectral wave-guides | | | | |
|--|------------|------------|------------|-------------|
| Shape 1 | 6.38705867 | 7.65676809 | 9.11294713 | 10.23292227 |
| Shape 2 | 6.3850403 | 7.65926504 | 9.11794073 | 10.23394057 |

Finite lattices

Now that the software was tested for the solution of eigenvalue problems, it needed to prove its ability to handle simulations of heterogeneous domains, like in photonic crystals. The following results are tests where the harmonic wave equation is solved for a finite grid of 4×4 circular dielectric slabs with ratio $\frac{r}{a} = 0.2$ and dielectric constant $\epsilon_r = 8.9$ surrounded by air. Boundary

conditions are as in 6.14, this is, inside a rectangular metallic boundary like if in a wave guide. The expected result is to see concentration of field inside regions with higher ϵ . As well as lower natural frequencies than those produced by homogeneous medium due to the denominator $\sqrt{\mu\epsilon}$ in 6.15.

| Comparison of ω for finite grid of dielectric rods vs air for the same mesh. | | | | |
|---|------------|------------|------------|------------|
| m,n | 1,1 | 1,2 | 2,2 | 3,1 |
| Embedded rods | 0.77475487 | 1.19190369 | 1.46064033 | 1.58328716 |
| Air | 1.11074305 | 1.75637223 | 2.22176045 | 2.48458998 |

Note in table 6.2.1 that if frequencies found for the air filled case are multiplied by two (this domain is twice as big) and then squared, we get the same result as in 6.2.1. Figure 6.14 illustrates the difference between solving for an homogeneous and non-homogenous problems. The flexibility to easily model interfaces and to couple regions is one of the great advantages of using both the Finite Element Method and a vectorial formulation. Note that these are solutions that are hard to solve analytically.

6.2.2 Bloch periodic lattices and dispersion curves

Finally, we solved the harmonic equation for infinite crystals by defining Bloch periodicity boundary conditions over a unitary cell. Looping through combinations of phase changes at boundaries, allowed us to see the spectrum for the crystal given different incident plane waves defined by varying wave number \vec{k} . Dispersion plots shown in figures 6.16, 6.17, and 6.18 are made by taking only the perimeter of the irreducible Brillouin zone which is the minimal representation of the domain in frequency space. Figure 6.19 shows the complete representation of natural frequencies for the lattice given every combination of incident plane waves with wave number $\vec{k} = \vec{k}_x + \vec{k}_y$ inside a unitary cell. The results presented in figure 6.17 were made with the same conditions as those used by Joannopolous in page 68 of the book: **Photonic Crystals: molding the flow of light** [13] and agree with their findings. Apart from great similarity between the curves, our value of 31.41% for the gap-midgap ratio is close to the one reported by them of 31.4%.

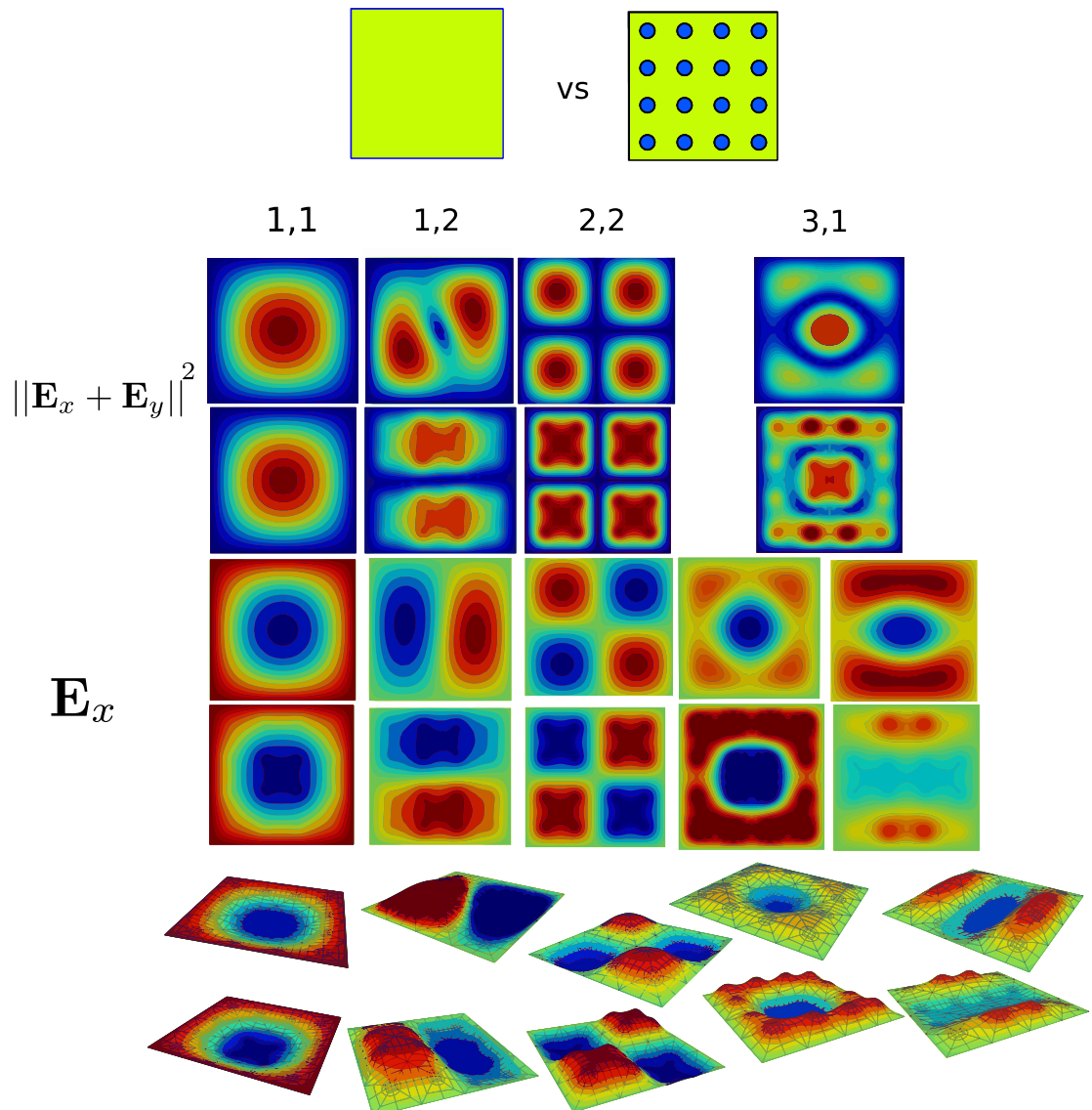


Figure 6.14: A lattice of dielectric rods embedded in a domain causes peaks of field magnitude in the places with higher dielectric constant.

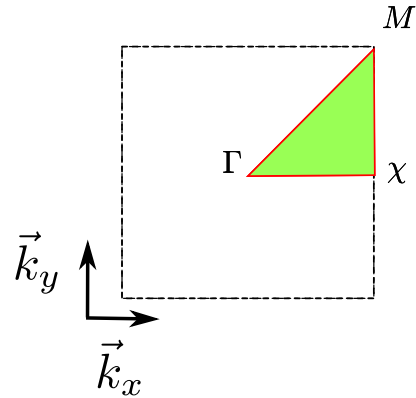


Figure 6.15: Illustration of reduced Brillouin zone in spectral domain, and reference points Γ , χ and M .

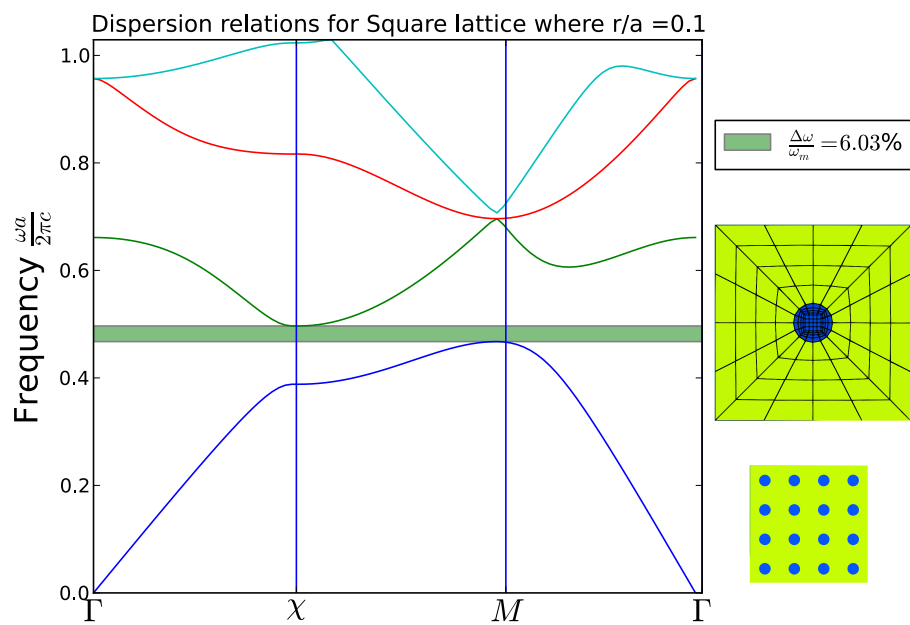
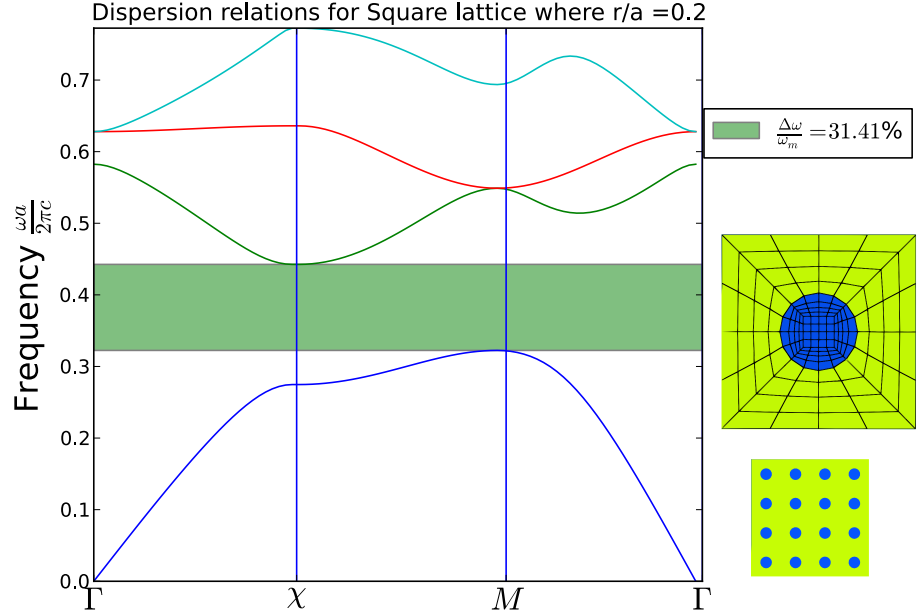
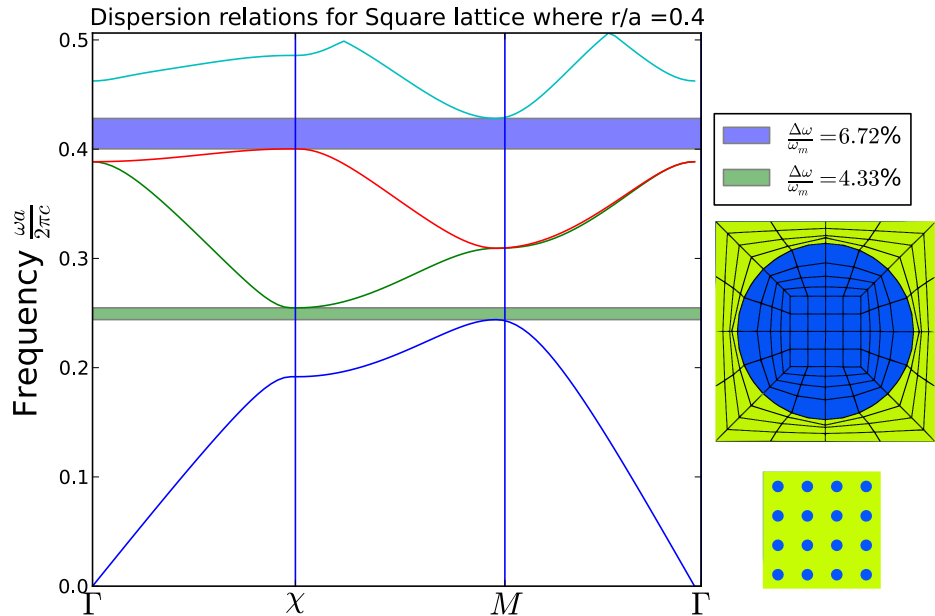


Figure 6.16: Dispersion plot for a square lattice of $r/a = 0.1$ and $\epsilon_r = 8.9$.

Figure 6.17: Dispersion plot for a square lattice of $r/a = 0.2$ and $\epsilon_r = 8.9$.Figure 6.18: Dispersion plot for a square lattice of $r/a = 0.4$ and $\epsilon_r = 8.9$.

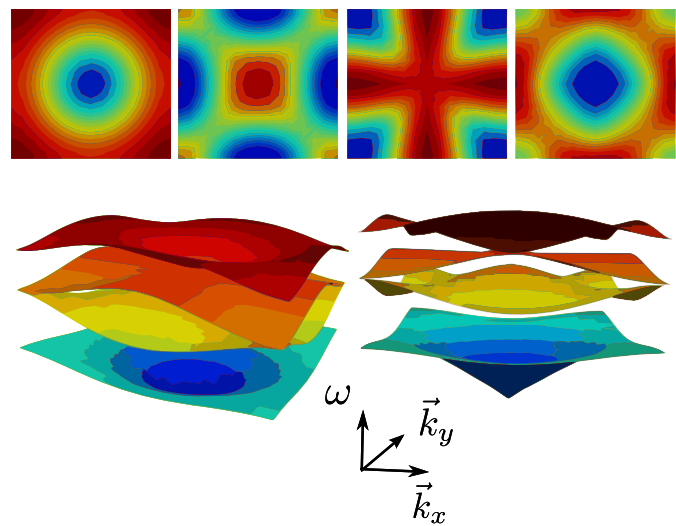


Figure 6.19: Frequency surfaces for square lattice of 6.17, where each point in a surface i represents the eigenvalue i of the solution, given a pair of \vec{k}_x , \vec{k}_y .

Chapter 7

Conclusions and future work

7.1 Conclusions

The necessary computational tools for the Finite Element modeling, simulation and analysis of EM wave propagation in the context of photonic crystals were developed as an ongoing open source software platform based on Python and structured around Object Oriented Paradigm. In order to build this platform, the necessary concepts and mathematical tools associated to the modeling of electromagnetic waves in periodic media were appropriated, specifically Maxwell's equations, and periodicity formulations taken from solid state physics.

Moreover, the finite element method was explored as an alternative to other methods commonly used in the analysis of PCs such as the Plane Wave Expansion (PWE) [28] method and Finite Differences Time Domain (FDTD)[19]. FEM was chosen mainly because it has proven to be a great general purpose method for investigating PCs [?] being its flexibility to model interfaces and defects in both frequency and spatial domains one of its greatest advantages. FEM is also well known for its stability and robustness and has proven its versatility in many fields of engineering.

The platform was designed using the Object Oriented Paradigm with having in mind the objective of having a well structured and flexible architecture, capable of being upgraded to future capabilities. Even though the architecture is in a developing stage and a proper manual for its use is pending, the modules, classes and methods that conform it are functional for production of results, and are documented for user reference. The reader is encouraged to visit the **online repository** and explore its examples.

Regarding the actual solution of problems, PeyeQM proved to be capable of accurately simulating 2D electromagnetism problems regarding stationary, and harmonic vector fields as well as fields inside in-homogeneous domains and infinite crystals. Time domain simulations (FETD) of finite lattices with point and line defects are still in developing phase but look very promising. The

need of CAD tools for the construction of finite lattices of dielectric rods with arbitrary size and placement was a factor that we sub estimated in the beginning. And quite a bit of time was spent on defining routines for the definition of clusters of dielectric regions within a rectangular matrix.

In the present time, we are working on fixing bugs, cleaning the code, and making a proper documentation of the software in order to achieve a product that can be shared and published as an article and or a downloadable application. This is a work that has great potential for academic and educational use by students of engineering and physics interested in diving into computational physics in the context of open source collaborative software.

7.2 Future work

The following is a list of items that are worth exploring in future work on PeyeQM platform:

- Definition of vectorial triangular elements for improving meshing flexibility and linear quadrilateral elements for computation speed. Triangular elements are simpler than quadrilaterals and are very often used by meshing algorithms in order to fill regions where quadrilateral elements get distorted. On the other hand, a comparison between convergence and speed between linear and quadratic elements would improve the understanding of the problem and ease calculations.
- Consider adding support for infinite boundary conditions for the simulation of unbounded domains. One popular candidate very often used in electromagnetism is the use of regions with Perfectly Matched Layers (PML)[\[12\]](#). Another possible implementation could be hybrid between FEM and Boundary Elements(BEM) as presented by Nicolás in [\[10\]](#).
- Evaluate convergence of the method for the problems described in chapter [6](#) using finer spatial and spectral (\vec{k} domain) meshes.
- Perform more simulations of time dependent problems involving defects in finite crystals. And compare the results of Q factor and efficiency with other publications.
- Integrate the CAD and solver into a optimization algorithm that maximizes transmission or confinement by inducing variations in position and shape of defects in the lattice.
- Consider parallelization schemes to be implemented in order to make bigger simulations plausible. Algorithms that split the computation into threads and take advantage of the parallel architecture of modern computers are the key to obtaining results of enormous simulation faster than before. Making research on things like weather and seismic simulation, molecular dynamics or drug compounds testing practical and realizable. With parallel a implementation of PeyeQM bigger domains and finer meshes would be able to be modeled in a robust workstation.

Bibliography

- [1] Hatice Altug. Ultrafast photonic crystal nanocavity laser. *Nature Physics*, 2, 2006. [9](#)
- [2] Imanol Andonegui. The finite element method applied to the study of two-dimensional photonic crystals and resonant cavities. *Optics Express*, 21:4072–4092, 2013. [51](#)
- [3] A.M. Apetrei and J.M. Moison. Electromagnetic field confined and tailored with a few air holes in a photonic-crystal fiber. *Applied Physics B: Lasers and Optics*, 2005. [9](#)
- [4] Filippo Capolino. *Theory and Phenomena of Metamaterials*. CRC Press, 2009. [8](#)
- [5] S. J. Chapman. Drums that sound the same. *The American Mathematical Monthly*, 102:124–138, 1995. [45](#)
- [6] David Keung Cheng. *Fundamentals of Engineering Electromagnetics*. Addison-Wesley, 1993. [37](#)
- [7] Santiago Echeverri. Implementación del método de elementos finitos para la ecuación de Schrodinger en estructuras periódicas. Unpublished project report, 2011. [9](#)
- [8] Nader Engheta. *Metamaterials: physics and engineering explorations*. Wiley Inter Science, 2006. [8](#)
- [9] Lawrence Cowsar Gang Bao. *Mathematical Modeling in Optical Science*. Society for Industrial and Applied Mathematics, 1987. [8](#)
- [10] Herbert Goldstein, Charles P. Poole Jr., and John L. Safko. *Classical Mechanics*. Addison-Wesley, 3 edition, 6 2001. [21](#)
- [11] Nicolás Guarín. Simulación Numérica de Problemas de Propagación de Ondas: Dominios Infinitos y Semi-infinitos. Master's thesis, Universidad EAFIT, 2012. [9, 52](#)
- [12] Ramón Rodriguez-Dagnino J. Gutierrez-Vega, S. Chávez-Cerda. Free oscillations in an elliptic membrane. *Revista Mexicana de Física*, 45:613–622, 1999. [44](#)
- [13] Jian-Ming Jin. *Theory and computation of electromagnetic fields*. Wiley, 2010. [9, 42, 52](#)
- [14] John D. Joannopoulos. *Photonic Crystals, Molding the Flow of Light*. Princeton University Press, 2008. [8, 15, 19, 46](#)

- [15] F.X. Kartner, S. Akiyama, and G. Barbastathis. Electronic Photonic Integrated Circuits for High Speed, High Resolution, Analog to Digital Conversion. *Proc. of SPIE*, 6125:612503–1, 2006. [9](#)
- [16] Yhefferson Gutierrez Loaiza. Estructura de bandas en un cristal fotónico bidimensional. Master's thesis, Universidad EAFIT, 2011. [9](#), [10](#)
- [17] Koshiba Masanori. Time-domain beam propagation method and its application to photonic crystal circuits. *Journal of Lightwave Technology*, 18:102–110, 2001. [9](#)
- [18] S.A. Moore. Photonic crystal laser with mode selective mirrors. *Optical Society of America*, 16, 2008. [9](#)
- [19] Salah Obayya. *Computational Photonics*. Wiley, 2011. [8](#)
- [20] Ardavan F. Oskooi, David Roundy, Mihai Ibanescu, Peter Bermel, J.D. Joannopoulos, and Steven Johnson G. Meep: A flexible free-software package for electromagnetic simulations by the FDTD method. *Computer Physics Communications*, 2009. [9](#), [51](#)
- [21] Nadia K. Pervez. Photonic crystal spectrometer. *Optics Express*, 18, 2010. [9](#)
- [22] Nannapaneni Narayana Rao. *Elements of engineering electromagnetics*. Pearson Prentice Hall, 2004. [42](#)
- [23] J.N. Reddy. *Applied Functional Analysis and Variational Methods in Engineering*. Krieger Publishing, 1 edition, 1991. [21](#)
- [24] Michael E. Plesha Robert D. Cook, David S. Malkus. *Concepts and applications of Finite Element Analysis Third edition*. John Wiley and Sons, 1989. [30](#)
- [25] Sara E. Rodriguez. Numerical Analysis of the Modal Coupling at low resonances ina a Colombian Andean Bandola in C using the Finite Element Method. Master's thesis, Universidad EAFIT, 2012. [9](#)
- [26] Vitaly Félix Rodriguez. Finite-Element Analysis of Photoinc Crystal Cavities: Time and Frequency Domains. *Journal of Lightwave Technology*, 23:1514–1521, 2005. [9](#)
- [27] Daniel E. Sierra. Desarrollo de un módulo computacional para la síntesis y procesamiento de campos ópticos con aplicaciones en holografía digital y speckle. Master's thesis, Universidad EAFIT, 2010. [10](#)
- [28] J. D. Steven G. Johnson, Joannopoulos. Block-iterative frequency-domain methods for Maxwell's equations in a planewave basis. *Optical Society of America*, 2001. [9](#)
- [29] John Joannopoulos Steven Johnson. Block-iterative frequency-domain methods for maxwell's equations in a planewave basis. *Optics Express*, 8:173–190, 2001. [51](#)
- [30] Edward Villegas. Modelización y Simulación de Efectos de Confinamiento en el Grafeno. Master's thesis, Universidad EAFIT, 2011. [9](#)

- [31] Pierre R. Villeneuve. Microcavities in photonic crystals: Mode symmetry, tunability, and coupling efficiency. *Physical Review B*, 54, 1996. [9](#)
- [32] Janik Wolters. Enhancement of the zero phonon line emission from a single nitrogen vacancy center in a nanodiamond via coupling to a photonic crystal cavity. *Applied Physics Letters*, 2010. [9](#)
- [33] E. Yablonovich. Photonic band structure: The face-centered-cubic case employing nonspherical atoms. *Physical Review Letters*, 67, 1991. [9](#)
- [34] Eli. Yablonovich. Inhibited spontaneous emission in solid-state physics and electronics. *Physical*, 58:2059–2062, 1987. [9](#)
- [35] Olgierd Cecil Zienkiewicz, Robert Leroy Taylor, and Jian Z Zhu. *The Finite Element Method: Its Basis and Fundamentals: Its Basis and Fundamentals*. Butterworth-Heinemann, 2005. [21](#)